Technical Report 1741
April 1997

High-T_c Superconducting Thick-Film Spiral Magnet: Development and Characterization of a Single Spiral Module

W. C. McGinnis T. E. Jones

Naval Command, Control and
Ocean Surveillance Center
RDT&E Division

San Diego, CA
92152–5001

DTIC QUALITY INSPECTED 4

19970530 067

Approved for public release; distribution is unlimited.

DISCLAIMER NOTICE

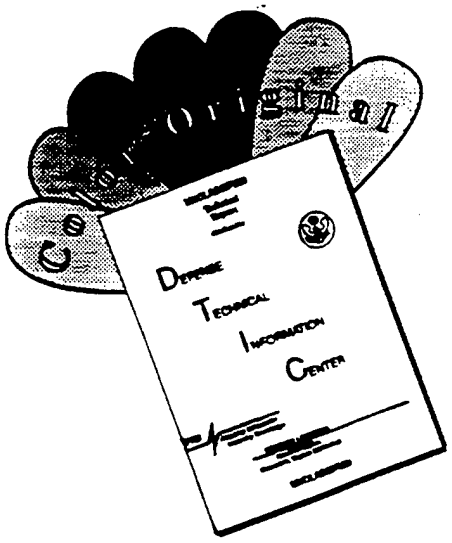

THIS DOCUMENT IS BEST QUALITY AVAILABLE. THE COPY FURNISHED TO DTIC CONTAINED A SIGNIFICANT NUMBER OF COLOR PAGES WHICH DO NOT REPRODUCE LEGIBLY ON BLACK AND WHITE MICROFICHE.

Technical Report 1741
April 1997

High-T_c Superconducting Thick-Film Spiral Magnet: Development and Characterization of a Single Spiral Module

W. C. McGinnis T. E. Jones

Naval Command, Control and
Ocean Surveillance Center
RDT&E Division

San Diego, CA
92152–5001

Approved for public release; distribution is unlimited.

NAVAL COMMAND, CONTROL AND OCEAN SURVEILLANCE CENTER
RDT&E DIVISION
San Diego, California 92152–5001

H. A. WILLIAMS, CAPT, USN
Commanding Officer

R. C. KOLB
Executive Director

ADMINISTRATIVE INFORMATION

The work detailed in this report was performed for the Office of Naval Research by the Naval Command, Control and Ocean Surveillance Center RDT&E Division, Materials, Sensors and Systems Branch, Code D364. Funding was provided under program element 0604561N.

Released by
I. Stevens, Head
Materials, Sensors and
Systems Branch

Under authority of
R. H. Moore, Head
Environmental Sciences
Division

This technology is related to the subject matter of one or more U.S. Patents assigned to the U.S. Government, including Patent No. 5,426,408, N. C. 75143. Licensing inquiries may be directed to:

Harvey Fendelman, Legal Counsel for Patents
NCCOSC Code D0012
San Diego, CA 92152–5765
(619) 553–3001

SB

EXECUTIVE SUMMARY

OBJECTIVE

The objective of this project was to make, experimentally characterize, and numerically model prototype modules of a new type of superconducting electromagnet based on stacked spirals of superconducting thick films instead of solenoid-wound wires.

RESULTS

The basic building block of the superconducting thick-film spiral magnet, consisting of a silver disk supporting a spiral-patterned $Bi_2Sr_2CaCu_2O_8$ thick film, has been produced using a melt-process technique. The magnetic fields generated by this single module, carrying currents of up to 60 A, have been measured at temperatures between 4.2 and 78 K. At currents below the critical current of the film, the axial field obtained per unit current is approximately 1.8 Oe/A. This measured field factor is in reasonably good agreement with a value of 1.4 Oe/A calculated using a simple computer model of the spiral magnet.

The crucial factors in producing a thick-film spiral module capable of generating such fields include: (1) film placement and patterning; (2) avoidance of substrate warping; (3) low-resistance, high-current contacts to the film; and (4) uniform melting of large area films. The best spiral films were produced by doctor-blading through a thin plastic stencil. Substrate warping was avoided by applying the thick-film pattern to both sides of the silver disk. High-current contacts were made with small pieces of silver foil embedded in the surface of the melted thick film. Uniform melting was obtained by assuring a uniform melt temperature across the substrate surface and by mixing a small amount of silver oxide with the $Bi_2Sr_2CaCu_2O_8$ powder before processing.

CONCLUSIONS

Using the techniques reported here, a high-field magnet based on multiple stacked modules of interconnected high-T_c spiral thick films can be constructed and successfully operated. The magnetic fields produced by such an arrangement meet or exceed those predicted by a simple computer model of the magnet. Based on the measured field factor of a single 3.2-turn, 5-cm diameter module, a 2-cm long stack of 100 such modules, with a current-carrying capacity of 50 A, would produce a maximum field of about 7.5 kOe. This, however, is not a limiting field for this magnet design, as much larger fields can be realized with higher current or by increasing the number of spiral turns.

RECOMMENDATIONS

Further progress toward a practical high-field magnet based on this spiral design will involve:

- Demonstration of a reliable interconnection between adjacent spiral modules.
- Selection/testing of a substrate material thermally matched to the high-T_c film (e.g., MgO).
- Use of buffer-layer films between the thick film and the substrate for chemical compatibility.
- Maximizing the current-carrying capacity of the high-T_c films by optimization of film application method, film oxygen content, and melt-processing procedures.
- Making a small working version of the spiral magnet (with 50 to 100 modules) using these materials and techniques (e.g., thin, silver-coated MgO disks alternated with high-T_c spirals).

TABLE OF CONTENTS

FIGURES

TABLE

INTRODUCTION AND BACKGROUND

The results of a project to make, experimentally characterize, and numerically model prototype versions of a new type of superconducting electromagnet are reported here. The so-called spiral magnet, based on superconducting thick films instead of wires, is described in the U.S. Patent entitled *Ceramic Superconducting Magnet Using Stacked Modules* (McGinnis, Jones, and Briggs, 1995), and in the section below, SPIRAL MAGNET DESCRIPTION AND MODELING. As a proof of concept, magnetic field data obtained from the basic building block of this magnet (a single module) is reported here, and is compared to predicted values of field generation based on a simple computer model of the magnet. Descriptions of the experimental techniques for making these prototypes, along with the results of measurements to characterize the superconducting materials used to build the modules, are also included. Finally, recommendations are made regarding the next steps in the further development of this new magnet.

Conventional iron-core electromagnets can produce magnetic fields only slightly in excess of 20 kOe,* and are large and heavy. Before the advent of superconducting magnets, the U.S. physicist Francis Bitter (1902-1967) devised a clever scheme to circumvent the 2-T saturation limit of the iron core used in a standard electromagnet (Bitter, 1936). The so-called Bitter magnet uses copper disks instead of copper wire as the conducting elements. The disks are in the shape of an annulus with a wedge cut out so they do not form a complete circle. The conducting copper disks are stacked vertically and insulated from one another except for connections at the wedge between adjacent disks. The geometry is similar to that of a spiral staircase. Current is introduced at one end of the magnet, flows around the first disk, continues around the second disk, etc., down the stack, and out the other end. Thus, the current flows around the stack in a helical fashion, just as in a wire-wound solenoid. The hole in the center of each copper disk forms the clear bore, or the magnetic field access region, of the magnet.

Like a superconducting magnet, the Bitter magnet uses no iron core; there is no "gain" from a high-permeability material. Unlike a superconducting solenoid, however, the geometric design required for the Bitter magnet to operate results in very inefficient use of electric current. The field factor, or ratio of magnetic field, H, produced per unit of current, is extremely low for a Bitter magnet, usually less than 10 Oe/A. For a commercial superconducting solenoid the field factor is typically around 1,000 Oe/A. To illustrate the practical effects of this difference, consider that for a typical small superconducting magnet, a current of approximately 80 A will produce a field of 80 kOe. To produce a magnetic field of 80 kOe with a Bitter magnet would take about 11,400 A. The consequences of this difference are enormous. An 80-A power supply is a simple rack-mounted item; 11,400 A requires a small power station. Also, the heat generated in the copper disks with such currents would melt the copper under ordinary conditions. To prevent a melt-down, extraordinary means are invoked in the design of the Bitter magnet. In addition to the center hole in each disk,

---

*The external magnetic field applied to a sample (by an electromagnet, for example) is usually referred to as the magnetic field strength, H. The units of H are oersteds (Oe) or ampere per meter (A/m). The magnetic field in the interior of a sample is denoted as the magnetic flux density, B, or magnetic induction. The units of B are gauss (G) or tesla (T). For a sample with magnetization M, the two fields are related by $B = H + 4\pi M$ (in cgs electromagnetic or in Gaussian units), or by $B = \mu_0(H + M)$ (in SI units with $\mu_0 = 4\pi \times 10^{-7}$ H/m). Conversions between the above units are given by 4π Oe = 10^3 A/m and 1 G = 10^4 T. See references for further details on units (Goldfarb and Fickett, 1985; Jackson, 1975a; Cullity, 1972a).

multiple additional holes are drilled in each disk to facilitate cooling by forced flow of cold water. The disks are also thick and spaced far enough apart that cooling water can effectively carry away the heat before a catastrophic failure occurs.

The Bitter magnet, though clever, must be considered a brute force approach to the generation of large magnetic fields. Unpractical for useful motors and generators due to its ravenous need for electric power, extensive cooling requirements, large size, and high cost, the Bitter magnet did provide the scientific community with its only source of high magnetic fields for research purposes before the development of superconducting magnets. Bitter magnets are still in use today, and new magnet designs combine Bitter and superconducting magnets in so-called hybrid magnets for specialized research purposes.

Conventional superconducting magnets using low-temperature superconductors (such as Nb_3Sn or NbTi) must operate at 4.2 K, an extreme cryogenic temperature that usually requires liquid helium as a coolant. This is very expensive and impractical for most applications. The magnet described in this report uses so-called high-temperature superconducting materials that can be melt-processed, which allows the magnet windings to be fabricated without requiring a wire form. Wires with high current-carrying capacity have proved to be extremely difficult to fabricate with the new ceramic high-temperature superconductors. The magnet described here is designed to operate in the general temperature range of 20 to 77 K, and, perhaps, even at higher temperatures, depending on the properties of the specific material used, using high-transition-temperature materials such as $Bi_2Sr_2CaCu_2O_8$ (Bi2212) or $Bi_2Sr_2Ca_2Cu_3O_{10}$ (Bi2223). Of course, it can also be operated at lower temperatures if desired.

SPIRAL MAGNET DESCRIPTION AND MODELING

DESIGN

The spiral magnet is designed to operate in a manner similar to that of a Bitter magnet (see INTRODUCTION AND BACKGROUND), but uses a superconducting thick film as the conductor rather than copper sheet. The film is fabricated in a flat, spiral pattern on a disk made of an appropriate material. Multiple disks are stacked vertically, and electrical (superconducting) disk-to-disk connections are made between the spirals. Each disk has a central hole that forms the clear-access bore in the final magnet. Two adjacent disks that form part of a spiral magnet stack are illustrated schematically in figure 1 (from the patent of McGinnis, Jones, and Briggs, 1995). The dimensions and relative proportions of the disks, 26, and spiral films, 16, are greatly exaggerated.

An example of a spiral-film pattern is illustrated in figure 2. Two spiral patterns, mirror images of each other, would be stacked alternately such that the current spirals first inward on one disk, outward on the next, and so on, as it goes down the stack of disks. The current circulation is always in the same rotational sense (see arrows 20 and 25 in figure 1). The spiral of figure 2 has three turns. However, in principal, one could use a single turn, or hundreds of turns, depending on the specifics of the design. The higher the number of turns per spiral (made with a thick film of a given cross-sectional area), the lower the actual current needed to generate a given magnetic field. The superconducting inter-disk connections are made at a through-holes, or vias, at the ends of the spirals.

With this design of interconnected spirals, rather large currents can be made to travel in a solenoidal fashion around each disk and down the stack, in a manner similar to that of a Bitter magnet. The individual disks can be quite thin and closely spaced. Like a Bitter magnet, no wire form of the conductor is required. Unlike a Bitter magnet, the current does not flow in entire sheets of the conducting material, but rather is made to flow in a spiral pattern on each disk. Also, unlike a Bitter magnet, no water cooling is required as no heat is dissipated in the magnet (as long as the film is superconducting). Cooling is required only to keep the superconducting material below its critical, or transition, temperature (T_c). Additionally, the field factor (in Oe/A) can be made quite high in this design, unlike the Bitter magnet, as the numerical examples in the subsection COMPUTER MODEL will illustrate.

Electrodynamically, the magnetic field generated by an infinitely long spiral magnet will be the same as that produced by an infinitely long wire-wound solenoid. The current, traveling in a solenoidal manner down a long stack of spiral-patterned disks,

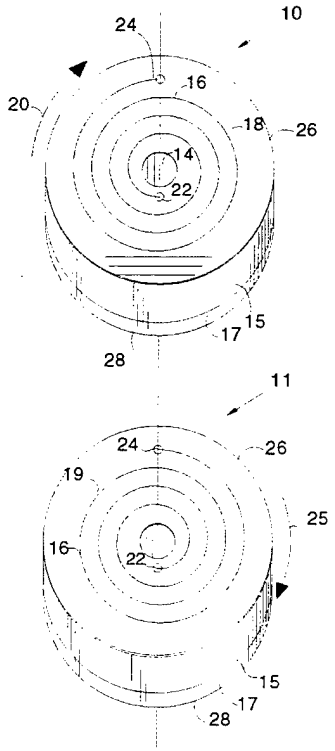

Figure 1. Schematic drawing of two adjacent modules in spiral magnet.

will produce, in the long-magnet limit, an interior magnetic field (for an empty magnet) given by $H = nI$, or a magnetic induction given by $B = \mu_o nI$ (SI units with I in amperes, n in turns per meter, H in amperes per meter, and B in tesla; Lorrain and Corson, 1970).* Here I is the circulating supercurrent and n is the number of current turns per unit magnet length. This expression for the field is identical to that produced inside a long wire-wound solenoid. In the wire-wound solenoid, the number n is simply the number of wire windings carrying the current, I, divided by the length of the solenoid. In the present design of spiral-patterned stacked disks, n is equal to the number of disks per unit magnet length times the number of spiral turns per disk. The two configurations are equivalent as far as the generation of a magnetic field well inside a long magnet is concerned. For a finite length magnet, the actual magnetic field produced is less than this long-magnet limit. Examples of actual computed field profiles for the spiral magnet are given below in the subsection entitled COMPUTER MODEL.

Figure 2. Three-turn spiral pattern (black) on substrate disk (gray).

MATERIALS

High-current wires made of high-T_c superconductors are under development, but are difficult to make (especially in long lengths) and are generally unavailable for winding magnets. However, these materials can carry very large currents in other forms. In particular, thin films of $YBa_2Cu_3O_7$ readily yield critical current densities (J_c) on the order of 10^6 to 10^7 A/cm^2 at liquid nitrogen temperature (Geerk *et al.*, 1989), and thick films of $Bi_2Sr_2CaCu_2O_8$ have J_c's in excess of 10^5 A/cm^2 at low temperatures, even in a magnetic field of 250 kOe (Kase *et al.*, 1990). The preferred high-temperature superconductors for the spiral magnet are Bi2212, with a T_c in the range of 80 to 90 K, and Bi2223, with a T_c near 105 K. These materials are appropriate for this magnet design because they can be melt-processed, orient readily with the high-current direction parallel to the substrate surface, and can carry high current densities. The Bi2212 phase has been chosen for this spiral magnet demonstration project because experiments to date have shown that maintaining phase purity after melt-processing is easier for Bi2212 than for Bi2223 (see review by Hellstrom, 1995). Another high-T_c superconductor, even one processed by other means, may ultimately prove a superior choice for this magnet design.

Of commonly available electrically insulating substrates, MgO is least reactive with Bi2212 (McGinnis and Briggs, 1992). Of conducting substrates, silver is one of the least reactive with the bismuth cuprate (Jin *et al.*, 1988; Balzorotti, *et al.*, 1992). Silver was chosen as the substrate material for making a prototype Bi2212 spiral film magnet because it is chemically compatible with Bi2212, relatively inexpensive, and is readily available in the form of thin, easily machined sheets.

---

* In mixed cgs and practical units, an equivalent expression for the magnetic field in the long-magnet limit is $H = 4\pi nI/10$ (H in oersteds, I in amperes, and n in turns per centimeter; Cullity, 1972b).

COMPUTER MODEL

A computer model has been developed to calculate the axial magnetic field profile that would be produced by a magnet using stacked, spiral-patterned disks. The FORTRAN-77 code is listed in appendix A. The starting point for the calculation is simply the known magnetic field H produced at an axial distance z from a ring of radius r carrying a current I. In SI units (with I in amperes and both r and z in meters), this field (in amperes per meter) is given by (Lorrain and Corson, 1970):

$$H = \frac{I r^2}{2\left(r^2 + z^2\right)^{3/2}} \quad . \tag{1}$$

Using a mixture of cgs and practical units (with I in amperes, and both r and z in centimeters), an equivalent expression for the field (in oersteds) is (Jackson, 1975b):

$$H = \frac{2\pi I r^2}{10\left(r^2 + z^2\right)^{3/2}} \quad . \tag{2}$$

This is a standard textbook result in electrodynamics that can be applied to the present geometry. Two approaches were used. First, the problem was solved by simply summing contributions from all the current rings (turns of the spiral) on each disk, and then from all disks along the length of the magnet. This results in a nearly exact calculation of the magnetic field along the axis of the magnet.* Second, a solution by integration was developed such that, as long as the density of disks along the axis is large, the magnetic field calculated is a good approximation to the more exact result. The tradeoffs are that the summation solution is more exact but numerically intensive, while the integration solution is a close approximation but very fast to compute. A crossover value for the number of disks (100) was determined such that the integration solution, employed for magnets with more than this number of disks, is within 1% of the summation solution (see appendix A).

Consider the following example. Assume design parameters (denoted here as "standard parameters") of 10 turns per spiral, a current density of 10^4 A/cm^2 in the superconductor, a superconductor thickness of 75 μm, disk spacing (top of one disk to top of adjacent disk) of 175 μm, spacing between spiral turns (open space between adjacent turns) of 1.3 mm, a clear bore of 2.5 cm, and an outer diameter of 20 cm. The resulting magnetic fields produced in the long solenoid limit are shown in table 1 for this and two other diameter magnets. The 20-cm diameter magnet produces a field of nearly 40 kOe with an actual current of about 55 A.

The computer model described here permits the calculation of actual field profiles for finite length magnets. Consider a 30-cm long (about one foot) version of the same magnet from table 1 that produces almost 40 kOe in the long magnet limit. The true field profile as calculated with this model is shown in figure 3. The actual maximum field, H_{max}, produced in the shorter magnet is about 37 kOe, or about 93% of the long-magnet limit. Note that the field factor for this design is almost 700 Oe/A, comparable to that of a commercial NbTi wire-wound superconducting solenoid, and about 100 times greater than that for a typical Bitter magnet. The profiles for magnets of various lengths, with otherwise standard parameters, are also shown in the figure.

---

*The only approximation used for this calculation is that the radius for a given spiral turn is taken to be the average of adjacent turns. For example, a 2-turn spiral, with a beginning radius of 1 cm and an ending radius of 3 cm, is modeled as two current rings with radii of 1.5 cm and 2.5 cm.

Table 1. Calculated magnetic fields in the long-magnet limit for 10-turn spiral magnets of various diameters and otherwise standard parameters (see text).

Magnet Diameter (cm)	Current (A)	Maximum Magnetic Field (kOe)
10	17.4	12.5
15	36.2	26.0
20	54.9	39.4

As seen in figure 3, the maximum field for a given configuration occurs at the center of the magnet. The value of this maximum field, for a magnet based on standard parameters, is plotted in figure 4 as a function of the number of disks (or magnet length). Also of interest in building a magnet of this design is the dependence of H_{max} on the disk spacing (for a given number of disks). This dependence is shown in figure 5 for magnets made with various number of disks and otherwise standard parameters. Note that for a small number of disks, the maximum field is essentially independent of disk spacing. In making a prototype magnet with a small number of disks, then, the disk thickness, which determines the disk spacing, is not critical.

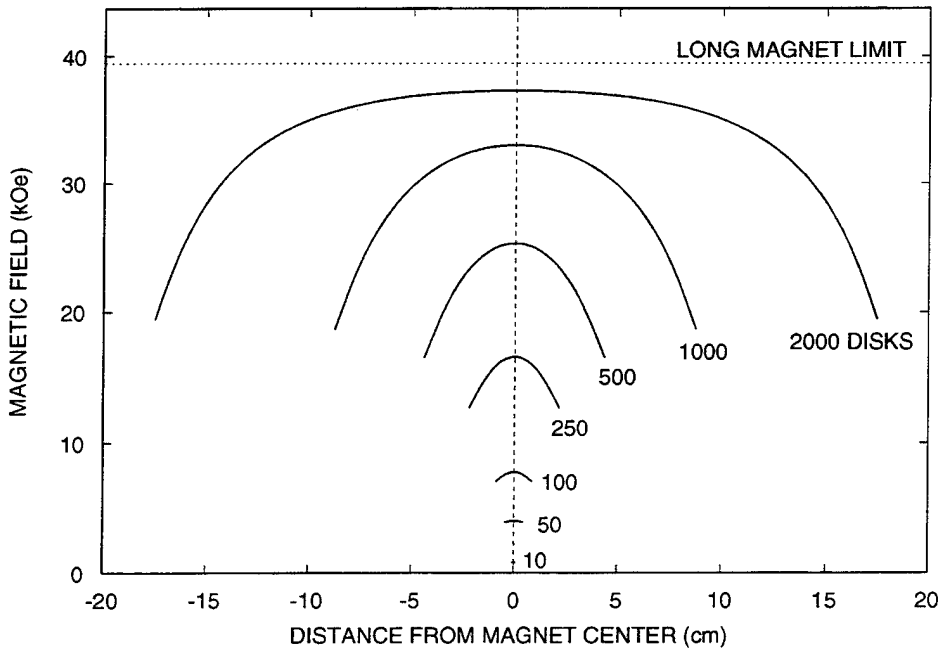

Figure 3. Calculated magnetic field profile, using standard parameters (see text), along the axes of 10-turn spiral magnets with various lengths (or number of disks). The magnet with 2000 disks is 35 cm long.

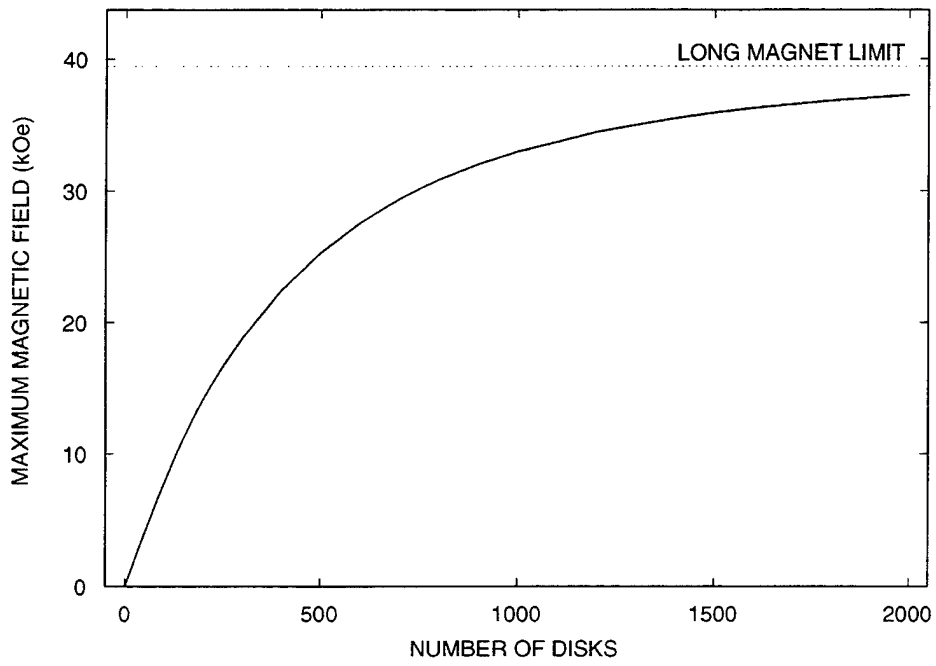

Figure 4. Calculated maximum magnetic field, using standard parameters (see text), at center of 10-turn spiral magnet as a function of the number of spiral disks used (that is, magnet length).

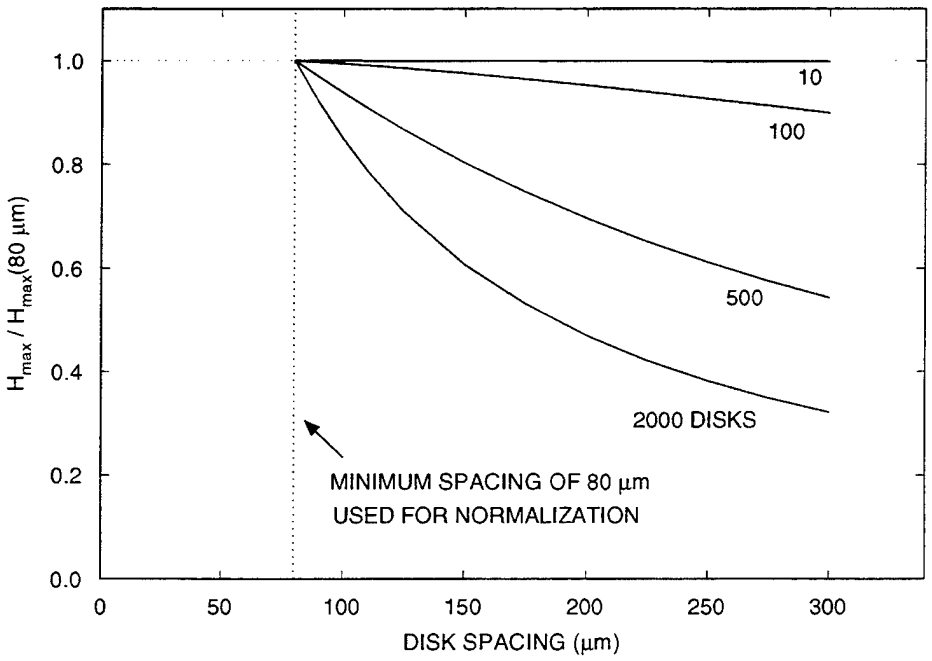

Figure 5. Calculated maximum magnetic field H_{max} (normalized to that for closely-spaced disks) versus disk spacing for a 10-turn spiral magnet with standard parameters (see text) and various number of disks.

EXPERIMENTAL METHODS

FILM AND SUBSTRATE PREPARATION

Bi2212 thick films were produced using a mixture of Bi2212 powder and polyethylene glycol (PEG), with the Bi2212:PEG weight ratio varying from 4:1 to 5:1. The mixture was then applied to an MgO or Ag substrate either spread by hand with a small implement, doctor-bladed with a small spatula, or screen printed through a polyester screen with a mesh size of 190 threads/inch (75 threads/cm). The Bi2212 powder, made by conventional solid-state reaction of oxides and carbonates of Bi, Sr, Ca, and Cu (McGinnis and Briggs, 1992), was thoroughly ground with a mortar and pestle before mixing with PEG.

A few of the Bi2212 films were processed on single crystal magnesium oxide (MgO) substrates (with an 001 orientation), but most were produced on 99.99% Ag-foil substrates with thicknesses ranging from 127 to 500 μm. Some Ag substrates were etched to form a track to confine the melted Bi2212 and, thus, define the film pattern. Details of the etching process are provided in appendix B. For other films, a pattern was defined only by the film placement on flat silver. In some cases, the film pattern was defined by Ag-painting a Ag foil template to the Ag substrate (and baking out the Ag paint at 500°C). The Bi2212 film was put on the flat silver surface exposed through the template. A variation on this technique is to attach a thin plastic (viewgraph) sheet, printed with the spiral pattern, to the Ag substrate using double-sided tape. The spiral track pattern is then cut from the sheet and removed from the substrate, leaving a plastic template. In addition to defining the spiral pattern, the template also serves as a stop for doctor-blading the film (troweling the Bi2212-PEG mixture onto the Ag exposed through the plastic template, which also serves as a spacer), thus giving a uniform film thickness, before melt-processing, of about 250 μm. This technique proved to be the easiest to implement and gave good results, even for samples with film spirals applied to both sides of the substrate. A Bi2212:PEG ratio of 4:1 by weight worked best for the doctor-bladed films.

The melt temperature of Bi2212 films prepared on Ag substrates is known to be about 20°C lower than that of films prepared on other substrates, such as MgO (Dietderich *et al.*, 1990). Ag, although it does not seem to react with the Bi2212, diffuses into the material from the substrate and lowers the melt temperature. Approximately 2 to 3 wt.% Ag can dissolve in the liquid formed when the Bi2212 melts (Margulies, *et al.*, 1996). In order in ensure uniform melting of the films produced here on Ag substrates, 2.5 wt.% Ag was sometimes added (as Ag_2O_2) to the Bi2212. The Bi2212 and Ag_2O_2 powder mixture was thoroughly ground before adding PEG. The silver oxide decomposes (at 100°C) to O_2 and elemental Ag while heating to the melt-process temperature. Films prepared in this way will be referred to as Bi2212+Ag films. Silver additions at this concentration have been shown to not degrade (and perhaps even enhance) the critical current density of Bi2212 (Jones *et al.*, 1992).

MELT PROCESSING

All of the Bi2212 and Bi2212+Ag films were melt-processed in air in a CM model 1700S-HTF single-zone tube furnace, with a 3-inch (7.6-cm) inner diameter, 30-inch (76-cm) long mullite tube. The tube has sealable end-caps, with gas flow and thermocouple feedthroughs. A type S (Pt/Pt-10%Rh) thermocouple, protected by a closed-end alumina tube, is positioned inside the furnace tube at its midpoint, where the samples are placed. A Eurotherm 818 temperature controller, in conjunction with another type S thermocouple placed next to the furnace's molybdenum disilicide heating elements (along the outside of the furnace tube), was used to program the processing cycle. The furnace specification for temperature uniformity is ±1°C over a 3-inch (7.6-cm) distance at the

tube center. Some samples were characterized after melt-processing by x-ray diffraction using a Rigaku RU-200B diffractometer with Cu Kα radiation.

In some cases, *in situ* measurements of four-probe sample resistance were made during the furnace processing. Teflon-insulated chromel (Ni-10%Cr) wires, fed through a sealed "tee" at the gas feedthrough of one of the furnace tube endcaps and crimped to small copper alligator clips, were clipped to 0.5-mm-diameter silver wires that went from the tube end-cap to the sample at the tube center. The silver wires were electrically insulated from each other by threading them through ceramic insulators. Fine gold wires (0.005-in., or 127-μm, diameter), silver painted to the silver wires and embedded in or silver-painted to the sample, were used to complete the connection. The sample resistance was measured with a lock-in amplifier using a phase-sensitive, low-frequency (about 200 Hz) ac technique.

LOW TEMPERATURE RESISTANCE VERSUS TEMPERATURE MEASUREMENTS

Small thick-film samples (less than 2.5 cm × 2.5 cm in area) were attached to the cold-finger of a helium closed-cycle refrigerator for resistance measurements, in vacuum, from room temperature down to as low as about 12 K. A thin layer of Apiezon N-grease between the sample and the cold-finger provided good thermal contact between the two. The sample temperature was measured by a Si-diode attached to the back of the cold-finger. Samples with Ag substrates were usually Ag-painted to a thin alumina sheet (to avoid electrical contact between the substrate and the cold-finger), which was, in turn, N-greased to the cold-finger. In this case, a differential thermocouple (copper-constantan-copper) was used to determine the temperature difference between the sample and the cold-finger. This temperature difference was combined with the diode temperature to give the sample temperature.

Larger samples (film spirals on 2-in., or 5.1-cm, diameter Ag foil disks) were mounted in a specially designed fixture (shown actual size in figures 6 and 7) attached to the end of a probe wired for use in a Janis SuperVaritemp liquid helium dewar. The probe includes multiple twisted-pairs of 34-gauge insulated copper wire for low-current/low-voltage connections to the sample, and to temperature and magnetic field sensors. The probe also has two high-current feedthroughs (Ceramaseal, with 3.9-mm diameter copper rod conductor rated at 60 A) that are connected to clamps on the sample fixture by braided copper tubing (spread open to enhance helium vapor cooling of the leads) The equivalent cross-sectional area of the braid is 1.2 mm^2, and the current-carrying capacity of the braid is rated at 19 A (in room temperature air). The two braided leads are insulated from each other and from the probe shaft by threading each one through polyethylene open-spiral cable wrap. This high-current lead system has been used, with no discernable sample temperature increase, up to a current level of 60 A with the sample in liquid helium, and up to 20 A with the sample in helium vapor. The helium evaporation rate has been calculated (based on Williams, 1963; see also Buyanov *et al.*, 1975) to be less than 50 ml/hr at a current of 20 A (with the sample in liquid helium at 4.2 K).

GENERATED MAGNETIC FIELD VERSUS CURRENT MEASUREMENTS

The dewar probe shown in figures 6 and 7 was also equipped with a Lake Shore Cryotronics model HGCA-3020 cryogenic Hall generator (or sensor) for measuring the axial magnetic field produced by the spiral magnet samples. The sensor was mounted on the probe such that the axial position of the Hall element could be adjusted (at room temperature) to accommodate magnet samples of different lengths. The sensor was operated either in an ac mode (using phase-sensitive detection) or a dc mode, both giving the same results. In the ac mode, a 340-Hz excitation current was provided by a Tektronix FG501 function generator, and the sensor voltage measured using an

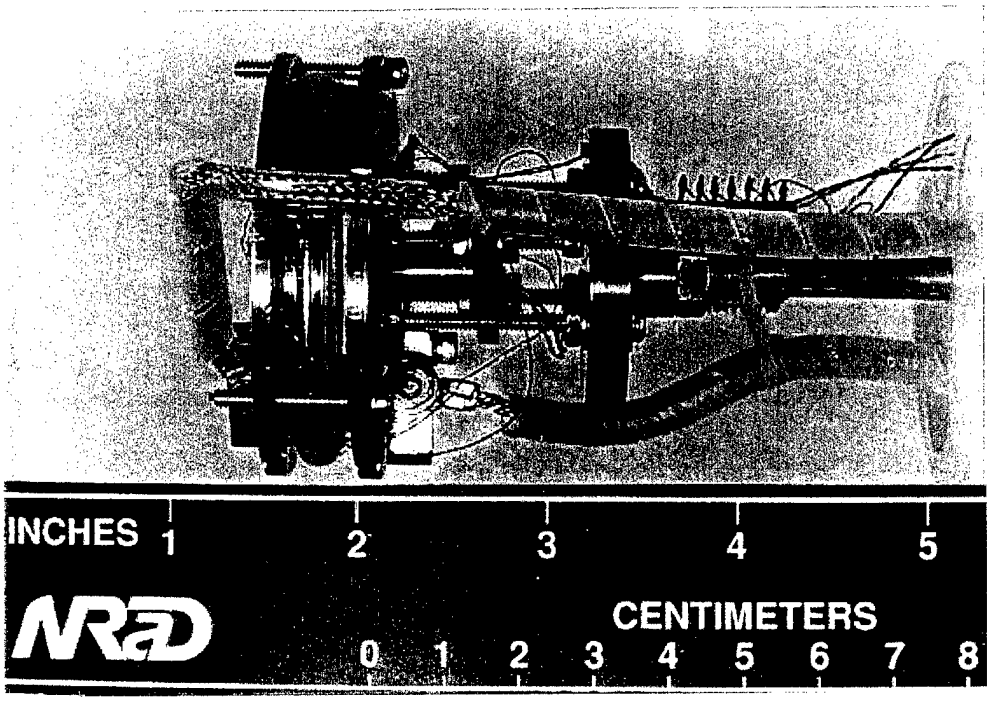

Figure 6. Fixture for cryogenic testing of spiral magnet (actual size).

EG&G Princeton Applied Research 124A lock-in amplifier. In the dc mode, a Keithley 225 current source and Keithley 181 nanovoltmeter were used. In both modes of operation the sensor excitation current was 100 mA. With zero current going through the spiral sample, the sensor produces a fixed (temperature dependent) voltage. The voltage-measuring instrument is then zeroed, corresponding to a measurement of zero magnetic field. Sensor voltage measured relative to this zero reference is proportional to the axial magnetic field produced by the spiral magnet. The proportionality factor for this Lake Shore sensor is 0.682 Oe/μV for an excitation current of 100 mA.

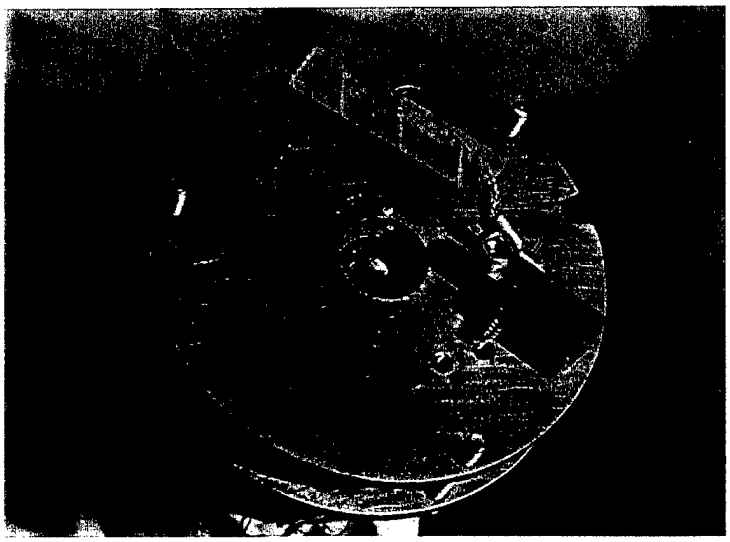

Figure 7. End view of test fixture for spiral magnet (actual size).

EXPERIMENTAL RESULTS

The results in this section are from samples ranging from simple Bi2212 films on small substrates to spiral films on larger, 2-inch (5.1-cm) diameter Ag disks. Also included are measurements performed on Cu-wire and Pb-film spirals. The order of presentation is chronological, with the results of the most recent, but more complex, spiral samples in the last part of this section (see Bi2212 THICK-FILM SPIRAL MAGNET MODULES).

Bi2212 THICK FILMS ON MAGNESIUM OXIDE SUBSTRATES

Magnesium oxide was chosen as the substrate for making *in situ* four-probe resistance measurements of Bi2212+Ag thick-film sample FCS341 during melt-processing in the furnace. These measurements were made to determine the melt and solidification temperatures of this film, and of subsequently processed Bi2212+Ag films prepared on Ag substrates. The results of this *in situ* measurement are presented in figure 8, which shows that the film melted at 868°C, and re-solidified at 865°C. The maximum resistance values measured correspond to saturation of the lock-in amplifier. This sample was heated from room temperature to 840°C at 300°C/hr, and then processed as follows:

$$840 \xrightarrow{30\ ^\circ C/hr} \overset{54\ min}{850} \xrightarrow{12\ ^\circ C/hr} \overset{12\ min}{880} \xrightarrow{12\ ^\circ C/hr} 830 \xrightarrow{300\ ^\circ C/hr} 25\,^\circ C \quad . \tag{3}$$

The furnace temperatures listed here and elsewhere in this report are measured temperatures (not necessarily equal to the programmed temperatures). As seen in the (low-temperature) resistance

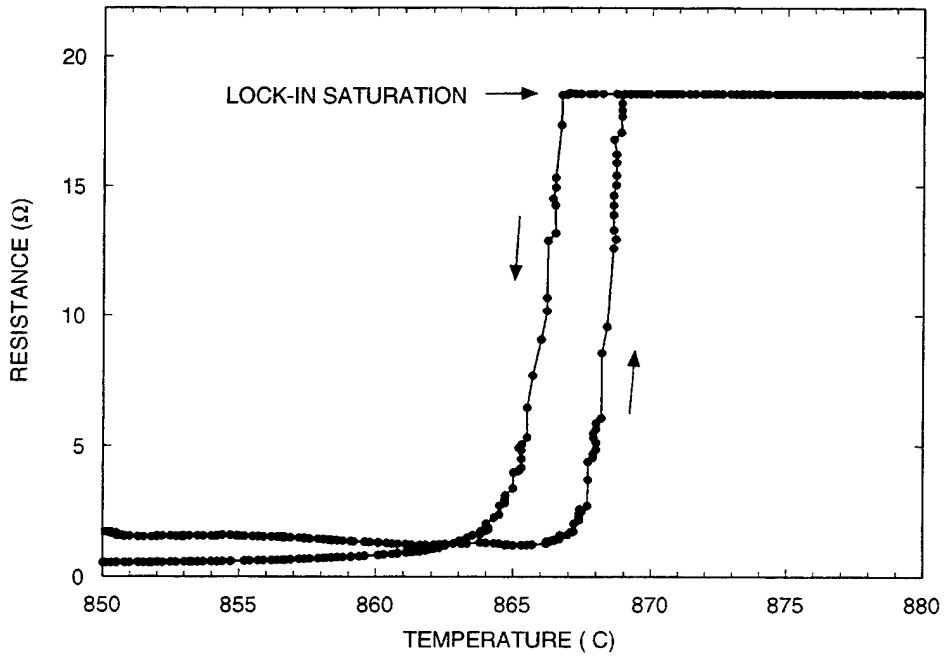

Figure 8. Resistance versus temperature as measured *in-situ* for Bi2212 thick film FCS341 on MgO substrate during melt-processing in furnace.

versus temperature plot in figure 9, this sample has a T_c of about* 83 K after the above furnace processing. Along with a bulk Bi2212 sample, this thick-film sample was then annealed at 600°C for 9.9 hr under Ar in order to improve the T_c by removing some oxygen from the compound (see appendix C for details). An increase in critical temperature should produce a corresponding increase in the critical current density at a given temperature. A higher critical current in turn would lead to higher achievable magnetic fields for a magnet made from the superconductor.

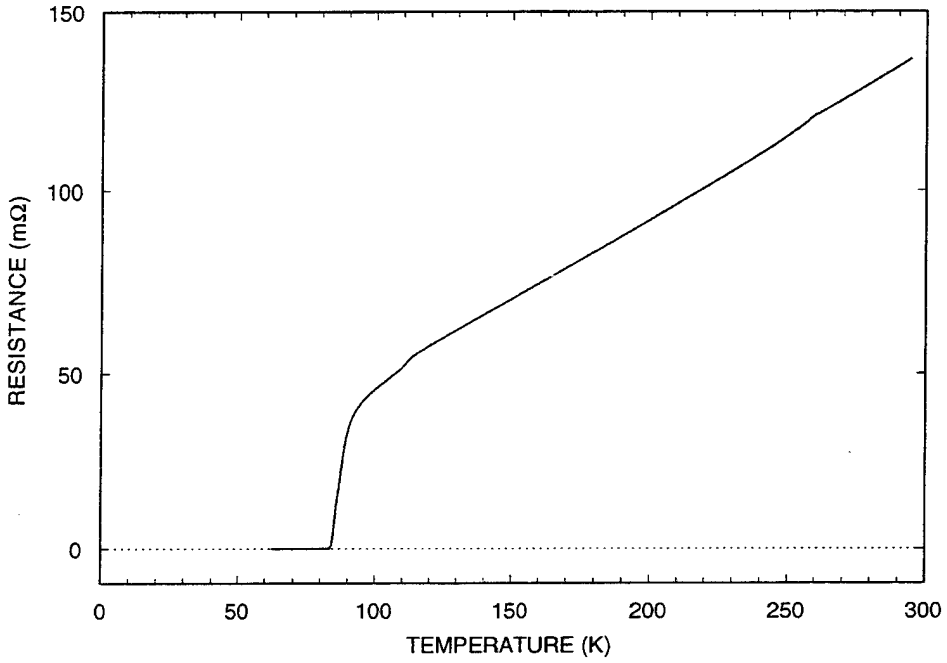

Figure 9. Low temperature resistance versus temperature data for Bi2212 thick film FCS341 on MgO substrate (after melt-processing).

Bi2212 THICK FILMS ON SILVER SUBSTRATES

Figure 10 shows the resistance versus temperature data (T_c = 83 K) for a doctor-bladed Bi2212 film (FCS328) on flat Ag that was heated to 874°C and melt-processed according to:

$$874 \xrightarrow{18\ \text{min}} \text{step} \xrightarrow{6\ \text{min}} 855 \xrightarrow{10\ °\text{C/hr}} 845 \xrightarrow{300\ °\text{C/hr}} 25\,°\text{C} \quad . \tag{4}$$

Note that because the electrical resistivity of Ag (1.59 μΩ-cm at 25°C; Boyer and Gall, 1985) is much less than that of Bi2212 in the normal state (a few mΩ-cm for polycrystalline samples at room temperature), resistance or resistivity measurements of Bi2212 films on Ag reflect mainly the properties of the substrate (when the film is not superconducting). The thickness of this film before and after processing was 170 μm and 130 μm, respectively. The x-ray diffraction data of figure 11

*Except as noted, the critical or transition temperature, T_c, is defined in this report to be the temperature at which the sample resistance goes to zero (for measuring currents much less than the critical current).

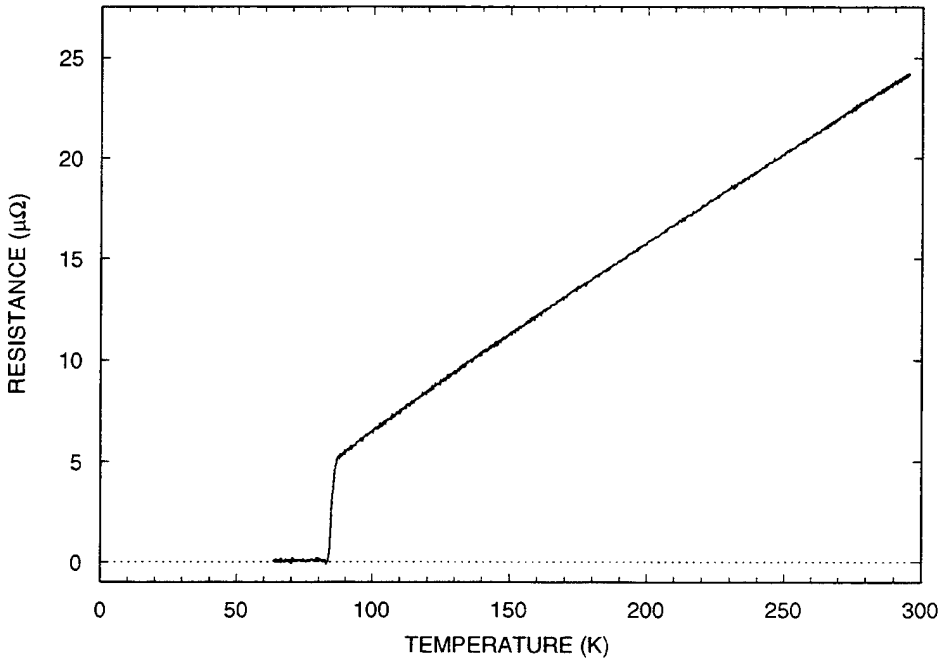

Figure 10. Resistance versus temperature data for Bi2212 thick film FCS328 on a silver foil substrate.

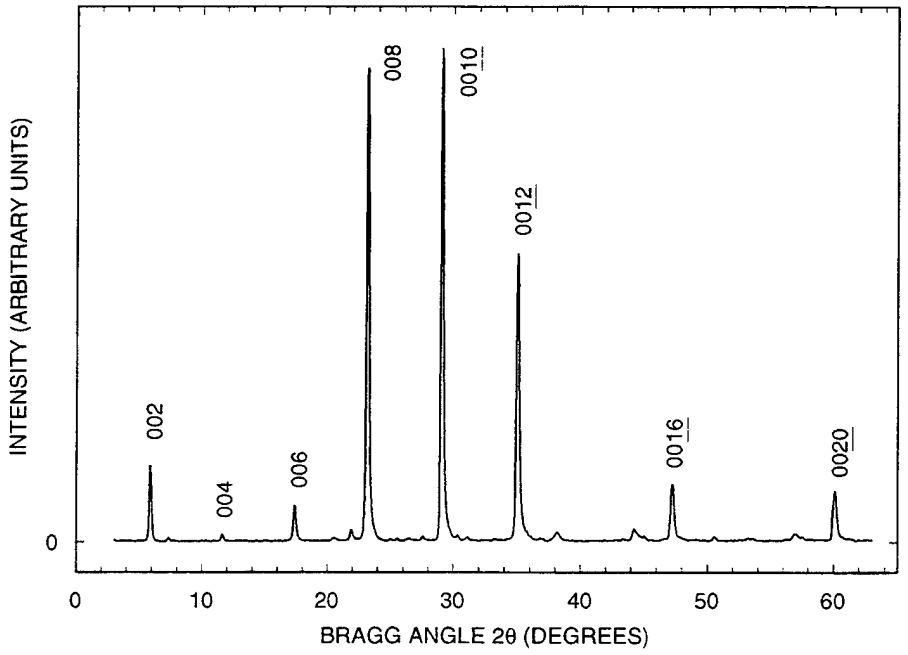

Figure 11. X-ray diffraction θ-2θ scan of Bi2212 thick film FCS328 on a silver foil substrate. The major 00ℓ peaks are labeled.

shows that, like Bi2212 thick films melt-processed on single-crystal MgO substrates (McGinnis and Briggs, 1992), films similarly-processed on polycrystalline Ag substrates also exhibit preferred

orientation or alignment. The alignment of the (00ℓ) planes of the Bi2212 unit cell parallel to the substrate is demonstrated by the much higher intensity of 00ℓ peaks compared to non-00ℓ peaks. Because the critical current is much higher along these planes than perpendicular to these planes (within each single-crystal grain; Martin *et al.*, 1989), such alignment leads to a higher critical current for the sample as a whole.

One drawback to using Ag as a substrate is that its thermal expansion coefficient (1.97×10^{-5} °C^{-1} at 25°C; Boyer and Gall, 1985) is about twice that of Bi2212 (1.04×10^{-5} °C^{-1} at 25°C; Emmen *et al.*, 1990). Once a Bi2212 film on top of a Ag substrate has been melted and re-solidified at about 880°C, both the film and the substrate are in a relaxed state (under neither compression nor tension). As they cool down toward room temperature, however, the Ag contracts more than the Bi2212. These unequal contractions place the film under compression and the substrate under tension, and cause the sample to bow or warp (unless constrained), with the middle higher than the edges. One way to avoid this bowing effect is to place similar Bi2212 films on both sides of the Ag substrate. The compressive and tensile forces are then symmetrically opposed, and the sample does not bow. Another way to prevent bowing is to firmly attach the bottom of the Ag substrate to a stiff surface that will not bend (at least not perceptibly). This latter method has been used for some small samples here by attaching them to an alumina sheet with Ag paint, which is then baked out in a 500°C furnace. In both cases, however, the film remains under compression and the substrate under tension on cooling to room temperature.

COPPER-WIRE SPIRAL MAGNET MODULE

As a simple way of testing the measurement fixture and magnetic field sensors of figures 6 and 7, a flat spiral coil of insulated 14-gauge copper wire was made and mounted in the fixture for room temperature measurements. This test also permitted verification of some of the spiral magnet

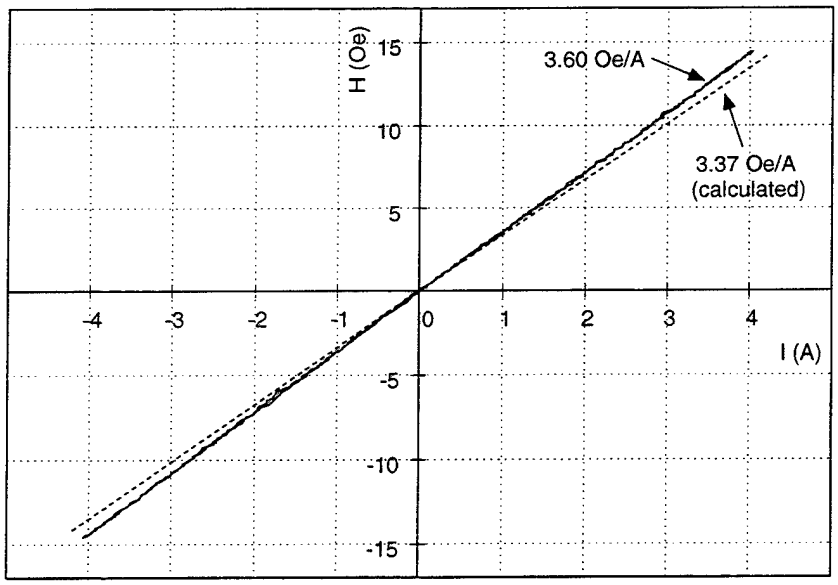

Figure 12. Generated (solid) and calculated (dashed) magnetic field for 7-turn copper wire spiral BLK2 versus applied current.

modeling predictions. The magnetic field generated by the room temperature coil as a function of applied current is shown in figure 12, along with the calculated values. The coil is pictured in figure 13.

Figure 13. Photograph of 7-turn copper wire spiral test module (sample BLK2). The dime coin at the bottom left is 1.85 cm in diameter.

LEAD-FILM SPIRAL MAGNET MODULE

In making a Bi2212-film spiral magnet module, there are a number of processing steps that need to be researched and optimized. Two examples are film production (binder selection, film application technique, pattern definition method, substrate preparation, etc.) and melt-processing (melt temperature and time, heating and cooling rates, anneal dwell times and temperatures, processing atmosphere, etc.). In order to test the basic concept of a magnet made from a superconducting spiral film on a conducting substrate, without the complications of these processing steps, a 3.2-turn spiral of lead (Pb) was melted onto a Ag disk substrate (see figure 14) and tested. The Pb thick film was melted with a soldering iron while the Ag disk was heated by a hot plate.

Another issue in producing a thick-film magnet is the method of making current connections to the film at the ends of the magnet. The connections must be mechanically strong and have a very low contact resistance. They should also be made directly to the film, rather than to the film via the Ag substrate. To understand this point, consider a film spiral on a single disk, with one current connection at the beginning of the spiral, and the other at the end of the spiral. Suppose that the connections consist of Ag tabs formed by cutting into the substrate next to the spiral beginning and end. The current is envisioned flowing from one tab, into the film, around the zero-resistance spiral, and out the other tab. However, if the resistance of the Ag substrate from one tab to the other is substantially less than the contact resistance between the substrate and the film, the current will flow

mainly through the substrate, and not along the spiral path of the film. Very little magnetic field would be generated in this case. If, instead, the current connections are made directly to the top of the film at the ends of the spiral, the current will be forced to flow through the connector-to-film contact and then around the zero-resistance spiral.

Current connections were, therefore, made directly to the top of the Pb film at the ends of the spiral, using a technique that could also be used for Bi2212-film spirals. A small rectangular piece of Ag foil (about 127 μm × 2 mm × 8 mm) was laid on top of the Pb film, which was then melted so that the Ag became embedded in the film, but with the top Ag surface exposed. The Ag piece did not directly contact the Ag substrate. A separate Ag foil tab (about 127μm × 2 mm × 20 mm) was bent into an "L" shape with legs that were 8 mm and 12 mm long. The short leg was soldered to the exposed surface of the embedded Ag foil piece using In-3%Ag solder, with the long leg projecting upward, perpendicular to the substrate disk. Two such connections were made, one at each end of the Pb spiral. When the disk was mounted in the fixture of figures 6 and 7, current connections were made to the Ag tabs extending from the disk using copper clamps as shown in figure 6. There is one clamp on one side of the fixture, and one on the other side. Both are electrically isolated from the fixture body using nylon shoulder washers.

The resistance versus temperature characteristics of this Pb-film spiral magnet module (denoted FLM61) are shown in figure 15. The superconducting transition of the Pb film at 7.15 K is shown in the inset. Measurements of magnetic field versus current were also made, both at 8 K (above the critical temperature, so that the film is normal), and at 5.1 K (such that the film is superconducting). These results are displayed in figure 16, along with the fields predicted by the computer model (dashed line with slope of 1.44 Oe/A). As expected, when the Pb film is not superconducting, very little field is generated (only that due to current flowing directly across the width of the Ag substrate). With the Pb spiral in the superconducting state, the resulting field is in fairly good

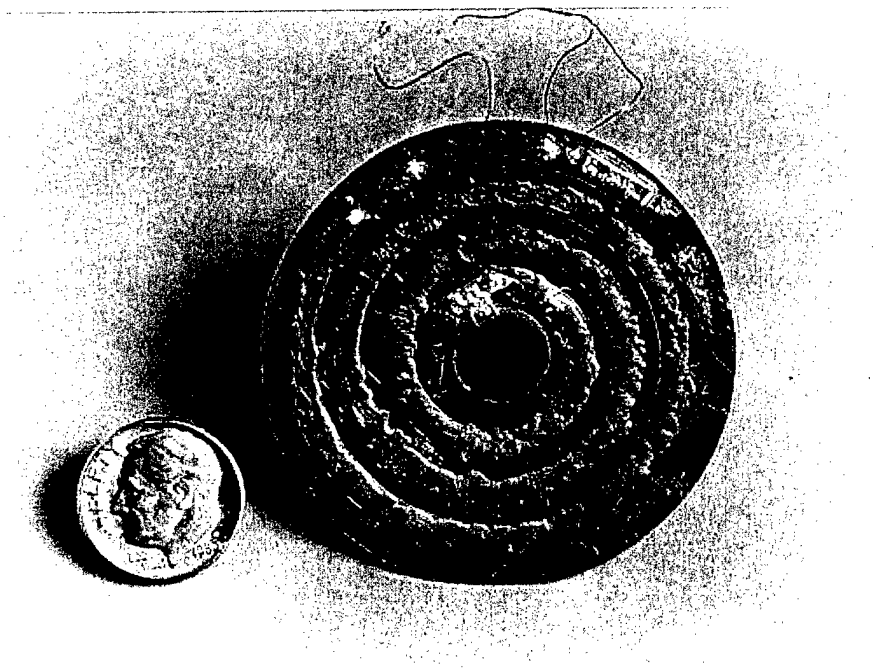

Figure 14. Photograph of 3.2-turn Pb thick-film spiral FLM61 on a silver disk substrate.

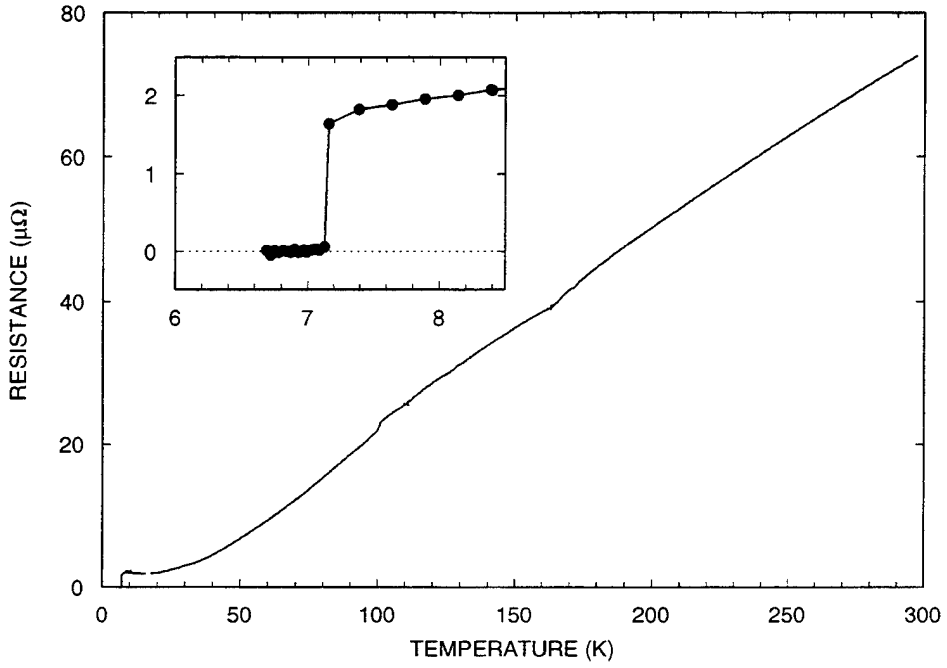

Figure 15. Resistance versus temperature data for Pb thick film FLM61 on a silver disk substrate. The inset shows the region of the superconducting transition.

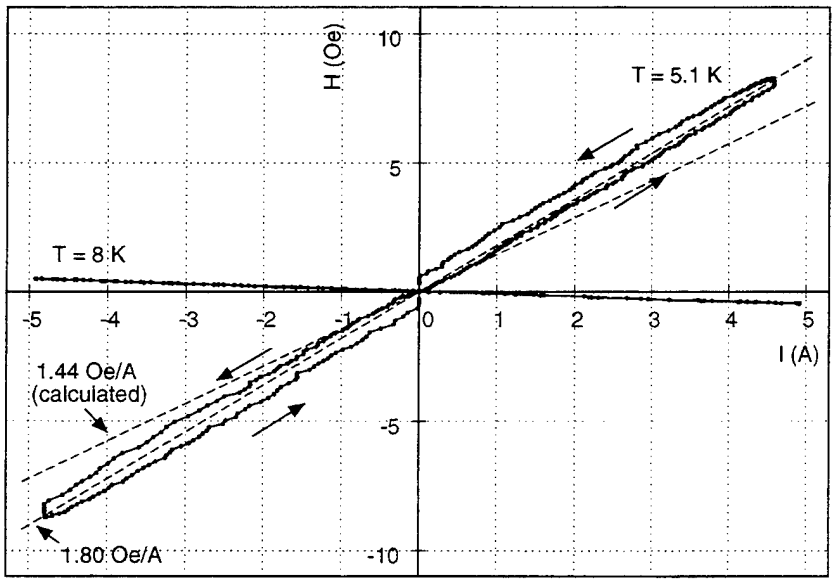

Figure 16. Generated magnetic field (solid) for 3.2-turn Pb spiral FLM61 versus applied current, both above and below T_c. Dashed line slopes are calculated and measured field factors.

agreement with the values calculated for a single 3.2-turn spiral. For these measurements, the current was swept by hand at an average rate of 130 mA/s, pausing for a few seconds at the extreme values.

The hysteresis observed in figure 16 occurs because the inductive impedance of the zero-resistance spiral forces some of the current through the low-resistance Ag substrate. That is, the superconducting spiral on Ag forms a parallel *LR* circuit with a time constant given by *L/R*, where *L* is the inductance of the spiral and *R* is the resistance of the Ag. The effect is the same for both Pb-film spirals and Bi2212-film spirals on Ag substrates.

Bi2212 THICK-FILM SPIRAL MAGNET MODULES

A number of Bi2212 spiral magnet modules were melt-processed, and their superconducting and magnetic-field-producing characteristics measured. Figure 17 is a photograph of a Bi2212+Ag sample (FCS359) that showed very good melting behavior. That is, the melted film had a uniform, dark-black, glassy appearance. This sample has a spiral on each side of the 500-μm-thick Ag substrate to avoid warpage during melt-processing. The film was applied by hand and the spiral pattern defined by Ag-foil stencils, as described in FILM AND SUBSTRATE PREPARATION. The spirals on opposite sides of the substrate were bridged by Bi2212+Ag that filled small holes drilled through the substrate (three holes on each end of the spiral), thus forming a continuous, melt-processed superconducting path between the spirals.

The measured furnace cycle for Bi2212+Ag spiral module FCS361, processed similarly to FCS359, is shown in figure 18. Heating to the melt temperature was done in steps in order to remove the PEG binder. The high temperature part of the cycle shown in the figure is:

$$\overset{30\ \text{min}}{874} \xrightarrow{18\ ^\circ\text{C/hr}} 867 \xrightarrow{30\ ^\circ\text{C/hr}} 863 \xrightarrow{300\ ^\circ\text{C/hr}} 25\,^\circ\text{C} \quad . \tag{5}$$

The superconducting transition for this sample is shown in figure 19. The R=0 critical temperature is 84 K. The resistance was measured along a short length on the outside turn of one of the spirals. This sample is similar to FCS359, but was made by doctor-blading through plastic stencils (see FILM AND SUBSTRATE PREPARATION). Looking down on the substrate, the rotational sense of both spirals for this sample is in the same direction. With the spirals connected at the ends, the current will be split evenly between the two. Therefore, for a given total current, the magnetic field expected from this sample should be the same as for a single spiral carrying the same total current. Electrical contact to the film was made in two ways. Voltage leads, and low-current (less than 100 mA) leads, consisted of fine gold wires embedded in the film before furnace processing. High-current leads (for conducting current around the spiral to produce the magnetic field) were made using the embedded-Ag-foil technique described for the Pb-film spiral magnet module. The specific resistivity of these current lead contacts was measured to be 9.5×10^{-6} Ω-cm^2 at 25 K. The thickness of the Bi2212+Ag film (on each side of the substrate) is roughly 350 μm, and the spiral turn width is about 3.4 mm.

The magnetic field produced by spiral sample FCS361 at 8.4 K, measured while hand-sweeping the current up and down from 0 to ±20 A, is plotted in figure 20. The experimental field factor of 1.8 Oe/A is in fair agreement with the model calculation of 1.4 Oe/A for a single 3.2-turn spiral with inner and outer radii of 7.2 mm and 22.2 mm, respectively. Based on this measured field factor, a 2-cm long stack of 100 such modules, with a current-carrying capacity of 50 A, would produce a maximum field of about 7.5 kOe (taking into account the effect of disk spacing on the generated field; see figure 5). This, however, is not a limiting field for this magnet design, as much larger fields can be realized with higher current or by increasing the number of spiral turns. Note the same

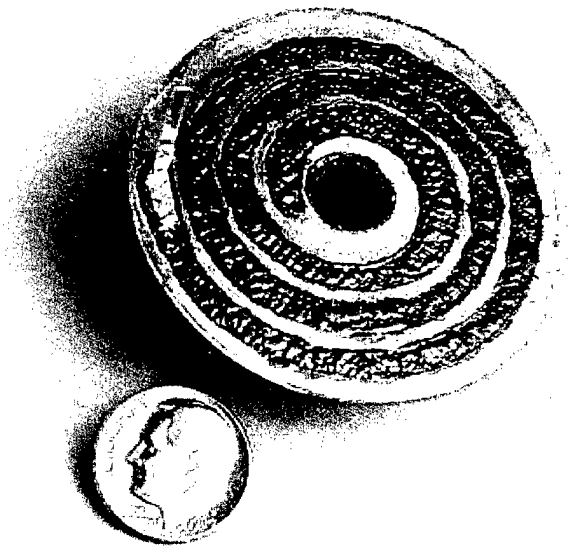

Figure 17. Photograph of Bi2212+Ag thick-film spiral FCS359 (on a silver disk substrate) that showed good melting behavior.

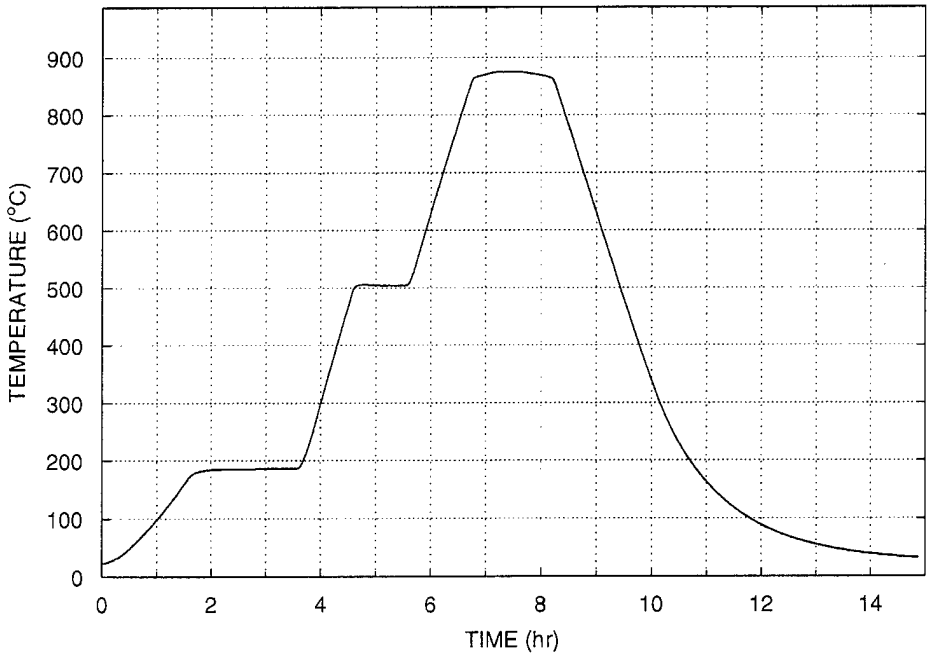

Figure 18. Elapsed time versus measured sample temperature during melt-processing of Bi2212+Ag thick-film spiral FCS361.

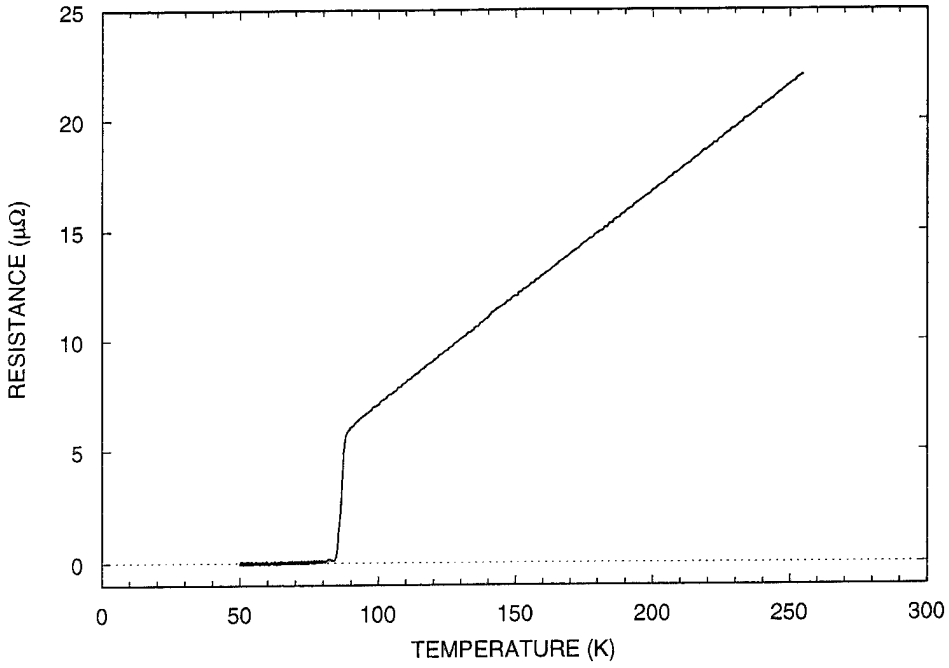

Figure 19. Resistance versus temperature data for Bi2212 thick-film spiral FCS361 on a silver disk substrate.

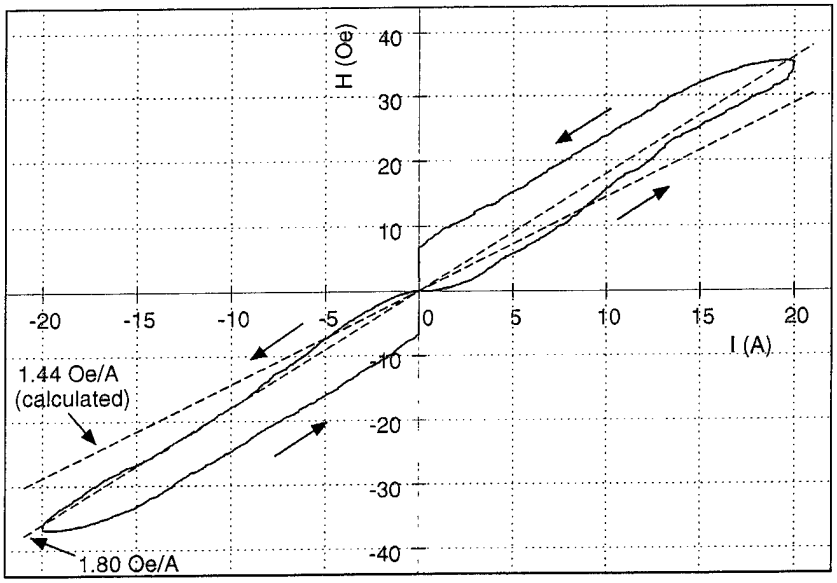

Figure 20. Generated magnetic field (solid curve) for 3.2-turn Bi2212+Ag spiral FCS361 versus applied current. Dashed line slopes are the calculated and measured field factors.

type of hysteresis in figure 20 as observed for the Pb-film spiral magnet module (figure 16). At even higher currents, the field generated by this single Bi2212 thick-film spiral will be limited by the intergranular critical current of the film. Once this critical current has been exceeded, the film starts to become resistive, and some of the current begins to flow through the low-resistance Ag substrate. The current that is shunted by the substrate does not travel in a spiral path, and so makes little contribution to the generated magnetic field.

This current shunting effect is seen in figure 21, where the data points indicate the steady-state field generated at 4.2 K (with the spiral sample in liquid helium) by the dc current levels shown. Based on this data (critical current I_c = 13 A), and the cross-sectional area of the films, the critical current density of FCS361 at 4.2 K is approximately 1.1×10^3 A/cm^2. Note that the processing parameters for this sample were not optimized to any extent, but were selected based on the visual appearance of large samples after melting (with limited number of trials, as described in the paragraph below). Further optimization of the melt-processing cycle for these Bi2212 spiral films should lead to substantial improvements in critical current density and, therefore, to increases in the maximum attainable magnetic field.

The current shunting effect also depends on temperature. Because the film's critical current decreases from its maximum value at low temperature to zero at T_c, the current value at which shunting starts to occur and, therefore, the saturation level of the generated magnetic field, both decrease with increasing temperature. This effect is seen in figure 22, in which the I versus H curves start to saturate at lower and lower values as the temperature increases above about 60 K. The current was ramped up and down (using a sawtooth waveform) from 0 to roughly ±5 A at a rate of about 60 mA/s.

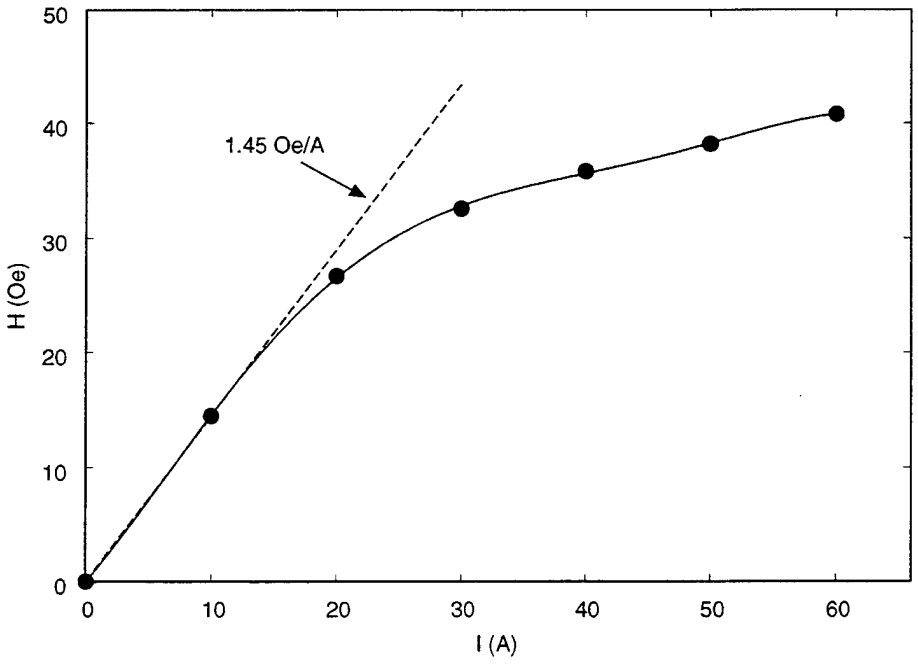

Figure 21. Steady-state magnetic field generated at 4.2 K by Bi2212+Ag spiral module FCS361 as a function of applied current. The solid line is a polynomial fit that serves as a guide to the eye.

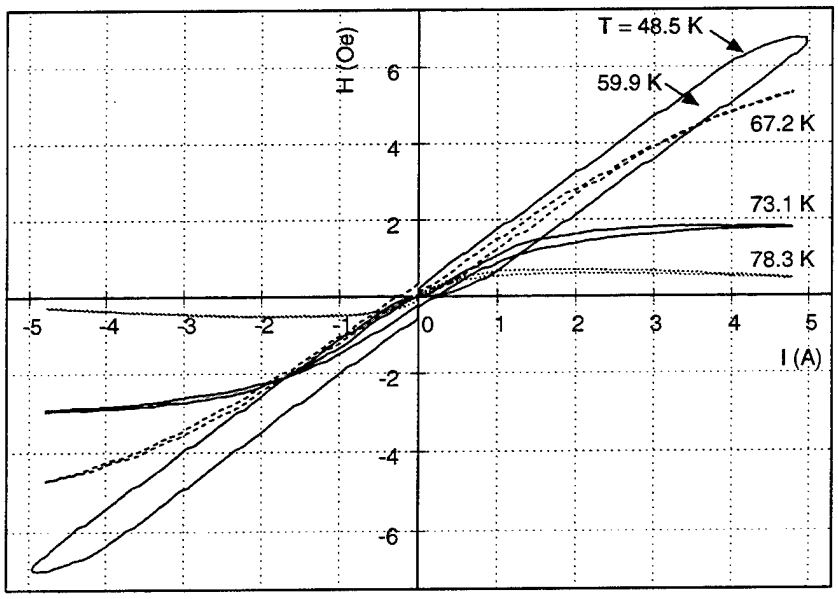

Figure 22. Generated magnetic field versus applied current at various temperatures for Bi2212+Ag spiral module FCS361.

One important factor in obtaining uniformly melted thick-film samples on large-area substrates is temperature uniformity across the sample during melt-processing. To investigate the conditions needed for uniform melting, test films of Bi2212+Ag on Ag substrates (film on one side of the substrate only) were inserted into the 865°C furnace, run through the melt cycle

$$865 \xrightarrow{30\ °C/hr} 873 \xrightarrow{60\ °C/hr} 865\,°C \quad , \tag{6}$$

removed from the furnace, and inspected. The insertion and removal was done in a few steps, over the course of several minutes, to avoid cracking the alumina dishes holding the samples. A Bi2212+Ag film on a small (1 cm × 1 cm) Ag substrate (FCS351) showed good melting behavior after the above processing cycle. The sample had been placed, film-side up, in the bottom of a small, rectangular alumina dish which, in turn, was placed in the center of the tube furnace. However, a spiral Bi2212+Ag film on a 2-inch (5.1-cm) diameter Ag substrate (FCS357) did not melt at all when processed in the same way. The non-melted appearance of a similarly processed 7-turn Bi2212 thick-film spiral (FCS336) is shown in figure 23. Sample FCS357 was subsequently processed three more times, each time raising the furnace temperature setting by 1°C and dwelling at that temperature for 12 minutes. After the first of these additional cycles (874°C), the film half on the left side of the furnace melted, but the right side of the film did not. After the 876°C cycle, a little more than half of the left-hand side looked like it had melted. However, some portions that had looked melted after the 874°C cycle now looked rough and somewhat depleted of film material. At this point, an inverted alumina tray was placed on top of the tray holding the sample (such that the sample was enclosed by the two trays), and the assembly placed in the center of the tube furnace. The sample was then processed at a furnace temperature setting of 874°C for 36 minutes. This time the film was uniformly melted along the whole length of the spiral, although it was somewhat dull black

in color rather than shiny black. Because of the film's multiple melt cycles at various temperatures and poor color, the superconducting properties of this film were not expected to be very good. Measurements of current versus generated magnetic field confirmed this expectation. As indicated by saturation of the generated magnetic field at relatively modest current levels (about 1 A), this film spiral has a very low critical current density, even at low temperature. Even so, for currents below 1 A the magnetic field generated by this 3.2-turn Bi2212+Ag spiral film coincides with that produced by the 3.2-turn Pb spiral film FLM61, with the field factor expected from the computer model. In addition to having undergone multiple process cycles with non-uniform melting, FCS357 may have also been degraded due to substrate bowing, which is evident in the oblique-angle view of the sample in figure 24. Sample FCS361, processed using the lessons learned from these test films, showed vastly improved characteristics (see figure 20) compared to FCS357.

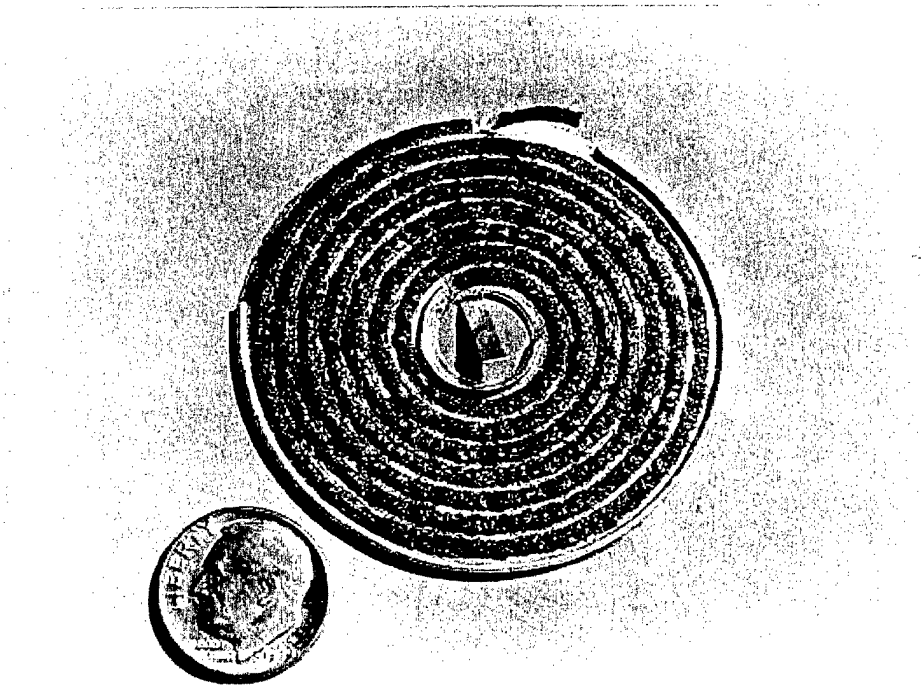

Figure 23. Photograph of 7-turn Bi2212 thick-film spiral FCS336. This sample did not appear to have melted after processing at 875°C for 12 minutes (compare to FCS359 of figure 17).

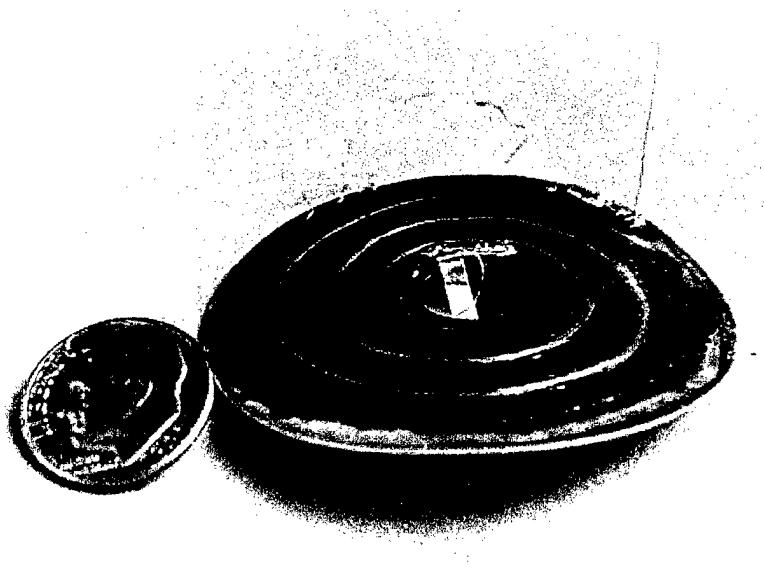

Figure 24. Photograph of Bi2212+Ag thick-film spiral sample FCS357 on a silver disk substrate. The oblique view shows the substrate bowing or warping effect due to thermal mismatch between the film and the substrate.

SUMMARY AND CONCLUSIONS

The basic building block or module of the superconducting thick-film spiral magnet, consisting of a single Ag disk supporting a spiral-patterned high-T_c Bi2212 thick film, has been produced by a melt-process technique. The magnetic fields generated by this single module, while carrying currents of up to 60 A, have been measured at various temperatures. At currents below the critical current, I_c, of the thick film, the field obtained per unit current flowing through the module is approximately 1.8 Oe/A. This measured field factor is in reasonably good agreement with the value of 1.4 Oe/A calculated using a simple model of the spiral magnet. For module FCS361, for example, I_c is about 4 A at 60 K, and 13 A at 4.2 K. For current values above I_c, the generated magnetic field starts to level off as the spiral film becomes resistive, and more and more current is shunted through the highly conductive Ag substrate.

Several factors proved to be crucial in obtaining a thick-film spiral module that is capable of producing the magnetic fields described in the above paragraph: (1) film placement and patterning; (2) substrate warping; (3) high-current film contacts; and (4) uniform melting of large area films. The best spiral films were prepared by doctor-blading a 4:1 by weight ratio of Bi2212+Ag powder (Bi2212 with 2.5 wt.% Ag) and polyethylene glycol through a thin plastic spiral-patterned stencil onto the Ag substrate. Substrate warping during furnace processing was avoided by applying the thick-film pattern to both sides of the Ag disk. Contacts to the film capable of carrying high currents (that is, contacts with very low resistance) were made with small pieces of Ag foil that become embedded in the film surface during melt-processing. Spiral films that show uniform melting across 2-inch (5.1-cm) diameter substrates were processed by encasing them within stacked alumina dishes, which, in turn, were placed in a tube furnace for the melting procedure. Uniform melting across the film thickness was enhanced by mixing Ag_2O_2 with Bi2212 powder, rather than relying on diffusion of Ag into the film from the surface of the substrate.

Although interconnection of two spiral modules with melt-processed Bi2212 was not demonstrated in this study, the spirals on opposite sides of a single module (FCS361) were connected by via holes drilled through the 50-μm-thick Ag substrate. The Bi2212+Ag film melted and filled these holes, providing a melt-processed, superconducting connection between the two spirals. Similar interconnections should be possible between modules of a multi-module spiral magnet.

Therefore, it is concluded that by using the techniques reported here, a high-field magnet based on multiple modules of interconnected high-T_c spiral thick films can be constructed and operated. Based on the measured field factor of a single 3.2-turn, 5-cm diameter module, a 2-cm long stack of 100 such modules, with a current-carrying capacity of 50 A, would produce a maximum field of about 7.5 kOe. This, however, is not a limiting field for this magnet design, as much larger fields can be realized with higher current or by increasing the number of spiral turns. The technical issues that need to be addressed to further accomplish this objective are outlined in the following section.

RECOMMENDATIONS FOR FURTHER DEVELOPMENT

This work has shown that a single spiral magnet module made using a high-T_c Bi2212 thick film on a Ag substrate can generate the magnetic field expected from numerical calculations. This is the first step toward realizing a practical high-field magnet based on the spiral design concept. Further progress toward this end will involve the following steps:

- Demonstrate the current-carrying ability of an interconnection between two spiral modules (Bi2212 on Ag), as evidenced by the magnetic field generated.

- Identify and test a substrate material (such as other oxides) with a thermal expansion coefficient closely matched to that of the thick-film superconductor. Promising candidate materials include MgO, nickel alloys, and some types of steel.

- Deposit Ag and/or MgO films on the thermally matched substrate as buffer layers between the thick-film superconductor and the substrate. Since these films must remain robust during melt-processing of the superconductor, intermediate adhesion-promoting films may be required.

- Maximize the current-carrying capacity of the Bi2212 thick films (on the buffered, thermally matched substrate) by optimizing the film application method, film oxygen content, and melt-processing procedures.

- Measure the magnetic fields generated by single and multiple module versions of the spiral magnet made using the combination of a thermally-matched substrate, buffer layer films, and superconducting thick films (both with and without an externally applied magnetic field).

- Make and characterize a small working version of a high-field superconducting spiral magnet (with approximately 50 to 100 interconnected spiral modules) using the materials and techniques listed above. This magnet might consist of thin, Ag-coated (for quench protection), polycrystalline MgO disks that are alternated with Bi2212+Ag spiral films (interconnected through vias in the disks). If required, the MgO disks could be manufactured by a ceramics company with a built-in track to contain the melt-processed thick film.

ACKNOWLEDGEMENTS

The authors gratefully acknowledge the following individuals for their contributions to this project: Scott Briggs (student contractor, investigation of silver etching techniques); Manjit Randhawa (visiting summer faculty, computer studies of spiral magnet performance, calculations for design of vapor-cooled leads for magnet fixture, help as mentor with Engineering and Science Residential Program (ESRP), and assistance with sample production and characterization); Pamela and Roger Boss (NRaD chemists, discussions on chemistry of silver etching process); and Robert Davis, Angela Schafer, and Tyler Watkins (high school students participating in ESRP, investigation of T_c-enhancement of Bi2212 by inert gas anneals).

The authors also acknowledge and thank the project sponsors Owen Ritter (Naval Surface Warfare Center, Carderock Division) and James Gagorik (Office of Naval Research).

REFERENCES

Balzarotti, A., F. Patella, F. Arciprete, N. Motta, and M. De Crescenzi. 1992. "Reactivity of the $Bi_2Sr_2CaCu_2O_8$ and $Bi_{1.7}Pb_{0.3}Sr_2CaCu_2O_8$ Surfaces for d-Metal Overlayers," *Physica C*, vol. 196, p. 79.

Bitter, F. 1936. "The Design of Powerful Electromagnets, Part I. The Magnetizing Coil," *Review of Scientific Instruments*, vol. 7, p. 482.

Boyer, H. E. and T. L. Gall (editors). 1985. *Metals Handbook, Desk Edition*, ch. 1, p. 47, American Society of Metals, Metals Park, OH.

Buyanov, Yu. L., A. B. Fradkov, and I. Yu. Shebalin. 1975. "A Review of Current Leads for Cryogenic Devices," *Cryogenics*, vol. 15, p. 193.

Cullity, B. D. 1972a. *Introduction to Magnetic Materials*, ch. 1, p. 15, Addison-Wesley, Menlo Park, CA.

Cullity, B. D. 1972b. *Ibid.*, ch. 2, p. 25.

Dietderich, D. R., B. Ullmann, H. C. Freyhardt, J. Kase, H. Kumakura, K. Togano, and H. Maeda. 1990. "Textured Thick Films of $Bi_2Sr_2Ca_1Cu_2O_x$," *Japanese Journal of Applied Physics*, vol. 29, p. L1100.

Emmen, J. H. P. M., W. J. M. de Kruijf, V. A. M. Brabers, and W. J. M. de Jonge. 1990. "Thermal Dilation of (Bi,Pb)CaSrCuO," *Physica C*, vol. 165, p. 293.

Geerk, J., G. Linker, and O. Meyer. 1989. "Epitaxial Growth and Properties of YBaCuO Thin Films," *Materials Science Reports*, vol. 4, p. 193.

Hellstrom, E. E.. 1995. "Processing Bi-Based High-T_c Superconducting Tapes, Wires, and Thick Films for Conductor Applications." In *High-Temperature Superconducting Materials Science and Engineering*, ch. 9, p. 383, D. Shi, Ed., Permagon, New York, NY.

Jackson, J. D. 1975a. "Appendix on Units and Dimensions". In *Classical Electrodynamics*, p. 811, John Wiley & Sons, New York, NY.

Jackson, J. D. 1975b. *Ibid.*, ch. 5, p. 178.

Jin, S., R. C. Sherwood, T. H. Tiefel, G. W. Kammlott, R. A. Fastnacht, M. E. Davis, and S. M. Zahurak. 1988. "Superconductivity in the Bi-Sr-Ca-Cu-O Compounds with Noble Metal Additions," *Applied Physics Letters*, vol. 52, p. 1628.

Jones, T. E., W. C. McGinnis, E. W. Jacobs, R. D. Boss, P. M. Thibado, J. S. Briggs, and W. E. Glad. 1992. "Effect of Silver Additions on Sintered $Bi_2Sr_2CaCu_2O_8$," *Physica C*, vol. 201, p. 279.

Kase, J., K. Togano, H. Kumakura, D. R. Dietderich, N. Irisawa, T. Morimoto, and H. Maeda. 1990. "Partial Melt Growth Process of $Bi_2Sr_2Ca_1Cu_2O_x$ Textured Tapes on Silver," *Japanese Journal of Applied Physics*, vol. 29, p. L1096.

Lorrain, P. and D. R. Corson. 1970. *Electromagnetic Fields and Waves*, ch. 7, p. 299, W. H. Freeman, San Francisco, CA.

Margulies, L., K. W. Dennis, R. J. Hofer, M. J. Kramer, and R. W. McCallum. 1996. "The Effect of Carbon on the Peritectic Melting of Bi2212 and Bi2212 + Ag," *Physica C*, vol. 264, p. 133.

Martin, S., A. T. Fiory, R. M. Fleming, G. P. Espinosa, and A. S. Cooper. 1989. "Anisotropic Critical Current Density in Superconducting $Bi_2Sr_2CaCu_2O_8$ Crystals," *Applied Physics Letters*, vol. 54, p. 72.

McGinnis, W. C. and J. S. Briggs. 1992. "Properties of $Bi_2Sr_2CaCu_2O_8$ Thick Films Melt-Processed at Temperatures Up to 950°C," *Journal of Materials Research*, vol. 7, p. 585.

McGinnis, W. C., T. E. Jones, and J. S. Briggs. 1995. "Ceramic Superconducting Magnet Using Stacked Modules," U.S. Patent No. 5,426,408.

Williams, J. E. C. 1963. "Counterflow Current Leads for Cryogenic Applications," *Cryogenics*, vol. 3, p. 235.

APPENDIX A: FORTRAN PROGRAM TO MODEL SPIRAL MAGNET

The following computer program, used to predict the magnetic field generated along the axis of the spiral magnet, is written in FORTRAN 77 and was compiled using the Ryan-McFarland compiler version 2.40. An example of the screen output for a 30-cm long magnet with standard design parameters (see COMPUTER MODEL in the SPIRAL MAGNET DESCRIPTION AND MODELING section) is shown after the program listing.

```
      PROGRAM MAGNET
C-----------------------------------------------------------------------
C   This program facilitates the design of the spiral magnet invented
C   at the Naval Command, Control and Ocean Surveillance Center, RDT&E
C   Division, by Wayne C. McGinnis, Thomas E. Jones, and J. Scott Briggs
C   ("Ceramic Magnet Using Stacked Modules," U.S. Patent No. 5,426,408).
C
C   Computation of the axial magnetic field inside the magnet is based
C   on the equation for the magnetic field "H" (in Oe) produced at an
C   axial distance "z" (in cm) from a ring of radius "r" (in cm)
C   carrying a current "I" (in amperes):
C
C      H = (2 pi I r**2)/[10 (r**2 + z**2)**(3/2)] ,  (pi = 3.14159...).
C
C   Each spiral turn on each module, or disk, is treated as a separate
C   current ring, with a radius equal to the mean radius of that spiral
C   turn.  The total field at a given position along the magnet axis
C   is found by adding up the contributions from all of the spiral
C   turn current rings.
C
C   For magnets with up to 100 disks, the axial magnetic field profile
C   is computed using the subroutine MAGSUM, which determines the field
C   by directly summing the fields due to each current loop.  For a
C   magnet with more disks, the magnetic field is computed using the
C   subroutine MAGINT, which uses integration of the above formula
C   along the magnet axis to find the total contribution of all spiral
C   turns of a given mean radius.  For disk spacing less than 300 micro-
C   meters, the field calculated by integration is within 1.0% of the
C   summation-determined field, and within 2% for SPACING less than
C   1000 micrometers.
C
C   The magnet design parameters can be saved to and recalled from a
C   configuration file.
C-----------------------------------------------------------------------
C   Written by:      T. E. Jones
C                    Jul 1993
C
C   Modified by:     W. C. McGinnis
C   Last modified:   8 Jan 1997
C-----------------------------------------------------------------------
      REAL*8 RMEAN(1000), HALF, PI, SPACING, CURRENT, HMAX
      REAL*8 DR, WIDTH, DEPTH, J, RINNER, ROUTER
      REAL*8 LENGTH, HLIMIT
      INTEGER*4 N, NDISKS, NSWITCH
      CHARACTER*20 OFILE, CFGFILE
      CHARACTER*1 ANS
      COMMON /PARAMS/ N, NDISKS, RMEAN, HALF, PI, SPACING, CURRENT, HMAX
      PI = 3.141592653589793D0
C  For number of disks NDISKS > NSWITCH, magnetic field H is computed
C  using the integration subroutine MAGINT, and otherwise using the
```

```
C  summation subroutine MAGSUM
       NSWITCH = 100
    50 WRITE (*,100)
   100 FORMAT (/'+Read parameters from a previously',
      1 ' saved configuration file? (y/n) ')
       READ (*,200) ANS
   200 FORMAT (A1)
       IF ((ANS .EQ. 'Y') .OR. (ANS .EQ. 'y')) THEN
          WRITE (*,300)
   300    FORMAT (/,'+Enter the configuration file name',
      1     ' (with extension): ')
          READ (*,400) CFGFILE
   400    FORMAT (A20)
          OPEN (UNIT=1,FILE=CFGFILE,STATUS='OLD',ERR=520)
          READ (1,500) N
   500    FORMAT (I8)
          READ (1,510) RINNER
   510    FORMAT (G12.4)
          READ (1,510) ROUTER
          READ (1,510) WIDTH
          READ (1,510) DEPTH
          READ (1,510) J
          READ (1,510) SPACING
          READ (1,510) LENGTH
          READ (1,500) NDISKS
          CLOSE (UNIT=1)
          IF (NDISKS .EQ. 1) THEN
             LENGTH = 0.D0
             SPACING = 0.D0
          ENDIF
          GOTO 1250
   520    WRITE (*,525)
   525    FORMAT (' No such file.  Please try again.'//)
          GOTO 50
       ELSE
   550    WRITE (*,600)
   600    FORMAT (/' Enter the number of spiral turns per disk, and',
      1     ' the radii'/' of the innermost and outermost spiral',
      1     ' turns in centimeters:'//
      1     '         N        R(INNER) (cm)       R(OUTER) (cm)'//)
          READ (*,*) N, RINNER, ROUTER
          WRITE (*,700)
   700    FORMAT (' Enter the spiral turn WIDTH in millimeters,',
      1     ' DEPTH in micrometers,'/
      1     ' and design current density, J, in A/cm**2:'//
      1     '              WIDTH (mm)     DEPTH (um)    J(A/cm**2)'//)
          READ (*,*) WIDTH, DEPTH, J
C  Convert WIDTH and DEPTH to cm
          WIDTH = WIDTH*1.D-1
          DEPTH = DEPTH*1.D-4
          WRITE (*,750)
   750    FORMAT (' You can enter either the NUMBER of disks',
      1     ' or the LENGTH of the magnet:'//
      1     '     RETURN an "N" to enter the NUMBER of disks'/
      1     '          or an "L" to enter the LENGTH of the magnet.'//)

          READ (*,200) ANS
          IF ((ANS .EQ. 'N') .OR. (ANS .EQ. 'n')) THEN
             WRITE (*,800)
  800        FORMAT (' Enter the number of disks:'/)
             READ (*,*) NDISKS
             IF (NDISKS .EQ. 1) THEN
```

```
               SPACING = 0.D0
            ELSE
               WRITE (*,810)
 810           FORMAT (' Enter the disk SPACING (top to top) in ',
     1          'micrometers:'/)
               READ (*,*) SPACING
C  Convert SPACING to cm
               SPACING = SPACING*1.D-4
C  Calculate magnet LENGTH in cm
               LENGTH = SPACING*DBLE(NDISKS - 1)
            ENDIF
         ELSE
            WRITE (*,900)
  900       FORMAT (' Enter the LENGTH of the magnet in',
     1       ' centimeters, and',
     1       ' the disk SPACING (top to top) in micrometers:'//
     1       '          LENGTH (cm)        SPACING (um)'//)
            READ (*,*) LENGTH, SPACING
C  Convert SPACING to cm
            SPACING = SPACING*1.D-4
C  Calculate number of disks in magnet
            NDISKS = IDNINT(LENGTH/SPACING) + 1
         ENDIF
      ENDIF
C  Calculate some necessary quantities from the input parameters
C
C  RMEAN(I) is the average radius of spiral turn I
  925 DR = (ROUTER - RINNER)/DBLE(N)
      DO 1000 I = 1, N
         RMEAN(I) = RINNER + DR*DBLE(2*I-1)/2.D0
 1000 CONTINUE
C  HALF is half of the magnet LENGTH
      HALF = LENGTH/2.D0
C  Calculate the actual CURRENT (in amperes) flowing through the magnet
      CURRENT = J*WIDTH*DEPTH
C  Calculate the magnetic field HLIMIT (in Oe) in the infinite
C  length magnet limit
      IF (NDISKS .EQ. 1) THEN
         HLIMIT = 0.
      ELSE
         HLIMIT = DBLE(N)*PI*CURRENT/2.5D0/SPACING
      ENDIF
      WRITE (*,1050)
 1050 FORMAT (//'+Enter output file name (with extension)',
     1 ' for storing'/' magnetic field vs. axial distance',
     1 ' from magnet center: ')
      READ (*,1100) OFILE
 1100 FORMAT (A20)
      OPEN (UNIT=1, FILE=OFILE)
      IF (NDISKS .GT. NSWITCH) THEN
         WRITE (*,1500)
         WRITE (1,1500)
 1500    FORMAT (' The following magnetic field profile was calculated'/
     1    ' using the integration routine MAGINT (because of the'/
     1    ' large number of disks) with the following parameters:'/)
      ELSE
         WRITE (*,1505)
         WRITE (1,1505)
 1505    FORMAT (' The following magnetic field profile was calculated'/
     1    ' using the summation routine MAGSUM (because of the'/
     1    ' small number of disks) with the following parameters:'/)
      ENDIF
```

```
      WRITE (*,1510) N, RINNER, ROUTER, 1.D1*WIDTH,
     1 1.D4*DEPTH, J, 1.D4*SPACING, LENGTH, NDISKS
      WRITE (1,1510) N, RINNER, ROUTER, 1.D1*WIDTH,
     1 1.D4*DEPTH, J, 1.D4*SPACING, LENGTH, NDISKS
 1510 FORMAT (' Number of spiral turns: ',I8/
     1 ' Inner radius:            ',G12.4,' cm'/
     1 ' Outer radius:            ',G12.4,' cm'/
     1 ' Width of each turn:      ',G12.4,' mm'/
     1 ' Depth of each turn:      ',G12.4,' um'/
     1 ' Current density:         ',G12.4,' A/cm**2'/
     1 ' Disk spacing:            ',G12.4,' um'/
     1 ' Magnet length:           ',G12.4,' cm'/
     1 ' Number of disks:         ',I8/)
      WRITE (*,1520) CURRENT, 1.D-3*HLIMIT
      WRITE (1,1520) CURRENT, 1.D-3*HLIMIT
 1520 FORMAT (' Calculated quantities:'//
     1 ' Actual current:                          ',G12.4,' A'/
     1 ' Field in long magnet limit:              ',G12.4,' kOe')
      WRITE (1,1550)
 1550 FORMAT (/' Axial distance (cm) from magnet center,',
     1 ' magnetic field (kOe):'/)
      IF (NDISKS .GT. NSWITCH) THEN
         CALL MAGINT
      ELSE
         CALL MAGSUM
      ENDIF
      WRITE (*,1725) 1.D-3*HMAX
 1725 FORMAT (' Maximum field for above configuration: ',G12.4,
     1 ' kOe')
      WRITE (*,1750) HMAX/CURRENT
 1750 FORMAT (' Field factor for above configuration:  ',G12.4,
     1 ' Oe/A'/)
      CLOSE (UNIT=1)
      WRITE (*,1200)
 1200 FORMAT (' Enter one of the following option numbers:'/
     1 '     1. Quit the program'/
     1 '     2. Run another case'/)
      READ (*,200) ANS
      IF (ANS .EQ. '2') THEN
 1250    WRITE (*,1300) N, RINNER, ROUTER, WIDTH*1.D1,
     1    DEPTH*1.D4, J, SPACING*1.D4, LENGTH, NDISKS
 1300    FORMAT (////////' The design parameters are:'//
     1    ' 1. # TURNS =  ',I8,'     spiral turns'/
     1    ' 2. R(INNER) = ',G12.4,' cm'/
     1    ' 3. R(OUTER) = ',G12.4,' cm'/
     1    ' 4. WIDTH =    ',G12.4,' mm'/
     1    ' 5. DEPTH =    ',G12.4,' um'/
     1    ' 6. J =        ',G12.4,' A/cm**2'/
     1    ' 7. SPACING =  ',G12.4,' um'/
     1    ' 8. LENGTH =   ',G12.4,' cm'/
     1    ' 9. # DISKS =  ',I8,'     disks'//
     1    ' Enter one of the following option numbers:'//
     1    '     1. Begin with an entire new set of parameters'/
     1    '     2. Change one parameter'/
     1    '     3. Run the program with currently selected parameters'/
     1    '     4. Quit the program'//)
          READ (*,200) ANS
          IF (ANS .EQ. '1') THEN
             WRITE (*,2000)
             READ (*,200) ANS
             IF ((ANS .EQ. 'Y') .OR. (ANS .EQ. 'y')) THEN
                WRITE (*,2100)
```

```
                READ (*,400) CFGFILE
                OPEN (UNIT=1,FILE=CFGFILE)
                WRITE (1,2200) N
                WRITE (1,2300) RINNER
                WRITE (1,2400) ROUTER
                WRITE (1,2500) WIDTH
                WRITE (1,2600) DEPTH
                WRITE (1,2700) J
                WRITE (1,2800) SPACING
                WRITE (1,2900) LENGTH
                WRITE (1,3000) NDISKS
                CLOSE (UNIT=1)
             ENDIF
             GOTO 50
          ELSEIF (ANS .EQ. '2') THEN
 1350        WRITE (*,1400)
 1400        FORMAT (/'+From above list of 9 parameters, enter',
     1        ' the number of the parameter'/
     1        ' that you wish to change (e.g., to change the',
     1        ' LENGTH, enter "8"): ')
             READ (*,200) ANS
             IF (ANS .EQ. '1') THEN
                WRITE (*,1410)
 1410           FORMAT (' Enter new number of spiral turns:'/)
                READ (*,500) N
             ELSEIF (ANS .EQ. '2') THEN
                WRITE (*,1420)
 1420           FORMAT (' Enter new inner radius',
     1           ' R(INNER) in centimeters:'/)
                READ (*,*) RINNER
             ELSEIF (ANS .EQ. '3') THEN
                WRITE (*,1430)
 1430           FORMAT (' Enter new outer radius',
     1           ' R(OUTER) in centimeters:'/)
                READ (*,*) ROUTER
             ELSEIF (ANS .EQ. '4') THEN
                WRITE (*,1440)
 1440           FORMAT (' Enter new spiral WIDTH in millimeters:'/)
                READ (*,*) WIDTH
C  Convert WIDTH to cm
                WIDTH = WIDTH*1.D-1
             ELSEIF (ANS .EQ. '5') THEN
                WRITE (*,1450)
 1450           FORMAT (' Enter new spiral DEPTH in micrometers:'/)
                READ (*,*) DEPTH
C  Convert DEPTH to cm
                DEPTH = DEPTH*1.D-4
             ELSEIF (ANS .EQ. '6') THEN
                WRITE (*, 1460)
 1460           FORMAT (' Enter new current density J',
     1           ' in A/cm**2:'/)
                READ (*,*) J
             ELSEIF (ANS .EQ. '7') THEN
                WRITE (*,1470)
 1470           FORMAT (' Enter new disk SPACING, in micrometers:'/)
                READ (*,*) SPACING
C  Convert SPACING to cm
                SPACING = SPACING*1.D-4
C  Calculate magnet LENGTH in cm
                LENGTH = SPACING*DBLE(NDISKS - 1)
             ELSEIF (ANS .EQ. '8') THEN
                WRITE (*,1480)
```

```
 1480          FORMAT (' Enter new magnet LENGTH in centimeters:'/)
               READ (*,*) LENGTH
               NDISKS = IDNINT(LENGTH/SPACING) + 1
            ELSEIF (ANS .EQ. '9') THEN
               WRITE (*,1490)
 1490          FORMAT (' Enter new number of disks:'/)
               READ (*,500) NDISKS
C  Calculate magnet LENGTH in cm
               IF (NDISKS .EQ. 1) THEN
                  SPACING = 0.D0
               ELSE
                  LENGTH = SPACING*DBLE(NDISKS - 1)
               ENDIF
            ENDIF
            GOTO 1250
         ELSEIF (ANS .EQ. '3') THEN
            GOTO 925
         ELSEIF (ANS .EQ. '4') THEN
            GOTO 1900
         ELSE
            GOTO 1250
         ENDIF
      ELSE
 1900    WRITE (*,2000)
 2000    FORMAT (/'+Save the currently selected parameters in a',
     1    ' configuration file? (y/n) ')
         READ (*,200) ANS
         IF ((ANS .EQ. 'Y') .OR. (ANS .EQ. 'y')) THEN
            WRITE (*,2100)
 2100       FORMAT (/'+Enter configuration file name',
     1       ' (with extension): ')
            READ (*,400) CFGFILE
            OPEN (UNIT=1,FILE=CFGFILE)
            WRITE (1,2200) N
 2200       FORMAT (I8,13X,'(number of spiral turns per disk)')
            WRITE (1,2300) RINNER
 2300       FORMAT (G12.4,' cm      (spiral inner radius)')
            WRITE (1,2400) ROUTER
 2400       FORMAT (G12.4,' cm      (spiral outer radius)')
            WRITE (1,2500) WIDTH
 2500       FORMAT (G12.4,' cm      (width of spiral turn)')
            WRITE (1,2600) DEPTH
 2600       FORMAT (G12.4,' cm      (depth of spiral turn)')
            WRITE (1,2700) J
 2700       FORMAT (G12.4,' A/cm**2 (current density)')
            WRITE (1,2800) SPACING
 2800       FORMAT (G12.4,' cm      (disk spacing)')
            WRITE (1,2900) LENGTH
 2900       FORMAT (G12.4,' cm      (magnet length)')
            WRITE (1,3000) NDISKS
 3000       FORMAT (I8,13X,'(number of disks)')
            CLOSE (UNIT=1)
         ELSE
            STOP
         ENDIF
      ENDIF
      STOP
      END
```

```
C-----------------------------------------------------------------------
      SUBROUTINE MAGSUM
C-----------------------------------------------------------------------
C   This subroutine calculates the axial magnetic field produced
C   inside a spiral magnet by summing the individual fields due to the
C   spiral turns of a given mean radius on all disks, and then summing
C   over all the spiral turns of different radii.
C-----------------------------------------------------------------------
      REAL*8 RMEAN(1000), HALF, PI, SPACING, CURRENT, HMAX
      REAL*8 C, Z(100), H
      INTEGER*4 N, NDISKS
      COMMON /PARAMS/ N, NDISKS, RMEAN, HALF, PI, SPACING, CURRENT, HMAX
      C = PI*CURRENT/5.D0
      DO 1400 I = 1,NDISKS
         Z(I) = -HALF + DBLE(I-1)*SPACING
         IF (DABS(Z(I)) .LT. 1.D-10) Z(I) = 0.D0
 1400 CONTINUE
C  Compute the magnetic field H (in Oe) at the axial position Z(I)
C  of each disk
      DO 1700 I = 1, NDISKS
         H = 0.D0
C  Sum over all spiral turns
         DO 1650 IR = 1,N
C  Sum over all disks.  At a given position Z(I), for given spiral turn
C  mean radius RMEAN(IR), compute H by summing along the length of the
C  magnet, adding contributions from all the other disks at positions
C  Z(IZ).
            DO 1600 IZ = 1,NDISKS
               H = H + C*RMEAN(IR)**2*
     1          (RMEAN(IR)**2 + (Z(I)-Z(IZ))**2)**(-1.5D0)
 1600       CONTINUE
 1650    CONTINUE
         WRITE (1,1675) Z(I), 1.D-3*H
 1675    FORMAT (G12.4,3X,G13.5)
C  The maximum magnetic field HMAX (in Oe) is at the magnet center
         IF (I .EQ. ((NDISKS + 1)/2)) HMAX = H
 1700 CONTINUE
      RETURN
      END
```

```
C-----------------------------------------------------------------------
      SUBROUTINE MAGINT
C-----------------------------------------------------------------------
C   This subroutine calculates the axial magnetic field produced
C   inside a spiral magnet by integrating over the individual fields
C   due to the spiral turns of a given mean radius on all disks,
C   and then summing over all the spiral turns of different radii.
C   For magnets with over 100 closely-spaced disks, the field calculated
C   by integration is within 1.0% of the summation-determined field
C   calculated in the subroutine MAGSUM.
C-----------------------------------------------------------------------
      REAL*8 RMEAN(1000), HALF, PI, SPACING, CURRENT, HMAX
      REAL*8 C, Z, H
      INTEGER*4 N, NDISKS
      COMMON /PARAMS/ N, NDISKS, RMEAN, HALF, PI, SPACING, CURRENT, HMAX
      C = PI*CURRENT/5.D0/SPACING
      DO 1700 IZ = -100,100,2
         Z = DBLE(IZ)*HALF/1.D2
         H = 0.D0
         DO 1575 IR = 1,N
            H=H+C*((HALF-Z)/SQRT(RMEAN(IR)**2+(HALF-Z)**2)+
     1        (HALF+Z)/SQRT(RMEAN(IR)**2+(HALF+Z)**2))
C  The maximum magnetic field HMAX (in Oe) is at the magnet center
 1575    CONTINUE
         IF (IZ .EQ. 0) HMAX = H
         WRITE (1,1600) Z, 1.D-3*H
 1600    FORMAT (G12.4,3X,G13.5)
 1700 CONTINUE
      RETURN
      END
```

The following magnetic field profile was calculated using the integration routine MAGINT (because of the large number of disks) with the following parameters:

Number of spiral turns:	10	
Inner radius:	1.250	cm
Outer radius:	10.00	cm
Width of each turn:	7.320	mm
Depth of each turn:	75.00	um
Current density:	0.1000E+05	A/cm**2
Disk spacing:	175.0	um
Magnet length:	30.00	cm
Number of disks:	1715	

Calculated quantities:

Actual current:	54.90	A
Field in long magnet limit:	39.42	kOe
Maximum field for above configuration:	36.63	kOe
Field factor for above configuration:	667.1	Oe/A

APPENDIX B: ETCHING OF SILVER SUBSTRATES

This appendix describes a chemical etching technique used to produce a spiral track in Ag disk substrates. The purpose of the etched track is to contain the melt-processed Bi2212 film. When a Bi2212 thick film is melt-processed on flat Ag, the Bi2212 material tends to spread somewhat beyond the pre-processed film boundary. This effect limits the separation distance between adjacent turns of a spiral-patterned film since the errant material could create a superconducting short between turns. For the Bi2212 spiral films on flat Ag investigated in this report, this between-spiral Bi2212 material was scraped away after furnace processing (it was relatively thin compared to the spiral portion of the film).

One way to avoid this film-spreading problem is to place the Bi2212 material in a track that has been cut or etched into the substrate surface. If the film thickness, as deposited, is less than the depth of the track, then the side walls of the track should prevent the processed film from spreading beyond the track edges. This arrangement also has the advantage that multiple spiral modules can be stacked on top of one another without the film on a lower module coming in contact with the bottom of the module immediately above it. In fact, if the individual module substrates are thick enough to permit a track on each side, then each module can accommodate two spiral films. This configuration would produce twice the magnetic field as a single-spiral module (for the same current), and would also avoid the substrate warping problem associated with single films on thermally mismatched substrates (see Bi2212 THICK FILMS ON SILVER SUBSTRATES, above).

The chemical etchant used was a so-called "triiodide" solution of potassium iodide, iodine, and water (with the molar content of KI greater than that of I_2). The etching process is thought to proceed as follows. KI dissolves in water as

$$KI\,(s) \longrightarrow K^+\,(aq) + I^-\,(aq) \quad . \tag{B-1}$$

The addition of I_2 to the KI solution causes the triiodide ion I_3^- to form (Peters *et al.*, 1974):

$$I_2\,(s) + I^-\,(aq) \longrightarrow I_3^-\,(aq) \quad . \tag{B-2}$$

The triiodide ions in turn react with the Ag substrate as

$$2Ag\,(s) + I_3^-\,(aq) \longrightarrow 2AgI\,(s) + I^-\,(aq) \quad , \tag{B-3}$$

causing a layer of AgI to form at the Ag surface. Further reaction at the Ag/AgI interface to form more AgI is controlled by the solution concentration of I_3^- (as determined by the amount of I_2 used) and its diffusion rate through the growing layer of AgI (see, for example, Dahan *et al.*, 1992). Meanwhile, the AgI at the AgI/liquid interface undergoes the following net complex-forming reaction with the I^- in solution (Cotton and Wilkinson, 1980; only the simplest complex is shown here):

$$AgI\,(s) + I^-\,(aq) \longrightarrow AgI_2^-\,(aq) \quad . \tag{B-4}$$

The AgI_2^- goes into solution. The Ag-I complexing reaction of equation B-4 proceeds at a slower rate than the AgI formation reaction of equation B-3. The net growth rate of the AgI film depends on the I^- concentration. If there is insufficient KI in the etching solution, then some AgI remains on the Ag substrate as a film covering the etched area. The thickness of this AgI film is governed by the competing processes of AgI formation at the Ag/AgI interface, and the removal of AgI at the AgI/solution interface.

The thickness of any remaining AgI film therefore depends, to first order, on the excess I^- concentration (the I^- concentration after formation of the triiodide ions). For a starting molar $KI:I_2:H_2O$ ratio of *a*:*b*:*c*, the excess I^- concentration would be given by the ratio (*a*-*b*):*c* (essentially all of the I_2 in equation B-2 forms I_3^-). In other words, equations B-1 and B-2 might be combined as

$$a \cdot KI + b \cdot I_2 \longrightarrow a \cdot K^+ + (a-b) \cdot I^- + b \cdot I_3^- \quad , \tag{B-5}$$

where (again, as a rough approximation) the second term on the right determines the AgI removal rate, and the third term on the right determines the AgI formation rate. Etchant solutions with a starting (*a*-*b*):*c* molar ratio greater than about 0.056 do not leave an AgI film after etching. However, profilometer roughness measurements showed that solutions that leave a very thin AgI film produce a smoother etched Ag surface than those that leave no AgI film. The remaining AgI film can be removed by ultrasonic agitation in a 1:23 molar (2:5 weight) solution of $KI:H_2O$.

Note that as etching proceeds, the I_3^- in solution becomes depleted as more and more of it is tied up as AgI (and then AgI_2^-). Therefore, the Ag etch rate will decline with time (even if reaction B-3 is not limited by diffusion), as evidenced by the decreasing slope seen in figure B-1. After the I_3^- is totally depleted, etching will stop at a limiting depth. For a given starting etchant volume and concentration, this limiting depth depends on the area of the surface being etched. The sample of figure B-1, SUB42, was etched with a solution consisting of 1.4361 g of KI, 0.7319 g of I_2, and 2.2864 g of water (a 3:1:44 molar ratio of $KI:I_2:H_2O$),* and had an etched area (defined by photoresist patterning) of about 1.65 cm^2. The etchant solution, which cools on mixing, was allowed to reach room temperature before etching began. The sample was removed from the etchant at the times shown, thoroughly rinsed with water, and dried. The average etched step height was measured (at the same location each time) using a Sloan Technology Dektak^{3}ST profilometer. A profilometer trace across the etched region of SUB42 (after 100 total minutes of etching) is shown in figure B-2. The average roughness at the bottom of the etched region in the figure was 0.32 μm. Sample agitation during etching was done every 5 minutes either by the act of removing/replacing the sample from the solution, or by gently swirling the solution by hand. The latter technique was found to give much more uniform and symmetric etching than, for example, by stirring or ultrasonic agitation. The beaker holding the etchant was covered with paraffin film to minimize iodine evaporative loss.

* Note that this etching solution is at least a factor of 10 more concentrated than that used in studies of AgI formation on Ag (Campbell *et al.*, 1986; Dahan *et al.*, 1992).

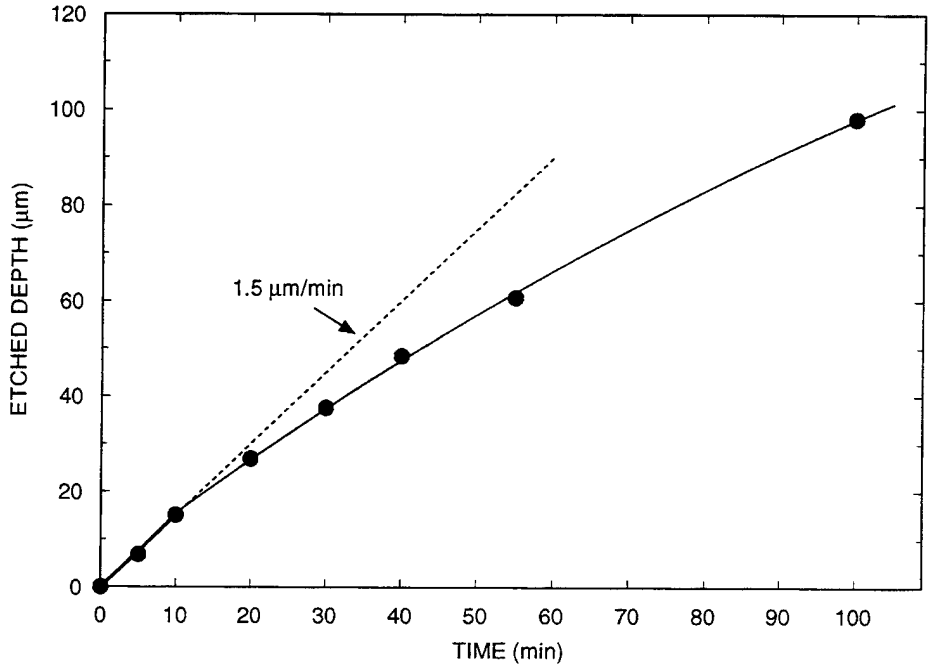

Figure B-1. Etched depth versus time for Ag foil SUB42 etched by a 3:1:44 molar ratio of KI:I_2:H_2O. The initial etch rate is indicated by the dashed line. The solid line is a guide to the eye.

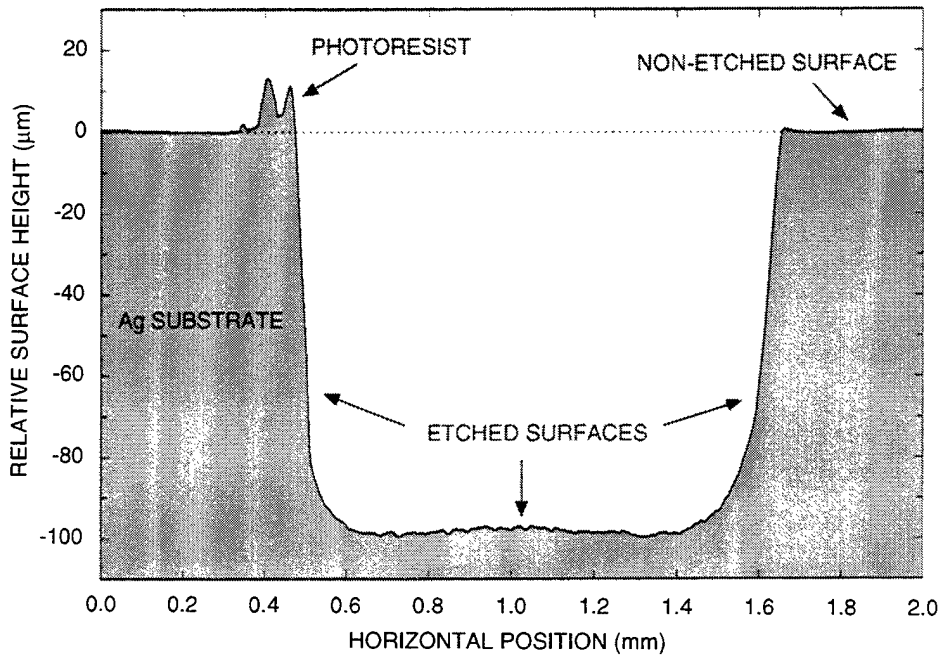

Figure B-2. Profilometer trace across etched region of Ag substrate SUB42. This sample was etched in a triiodide solution with a KI:I_2:H_2O molar ratio of 3:1:44 for a total of 100 minutes.

Figure B-3 is a micrograph of the profile of a Ag substrate sample (SUB22) that has been etched using the same procedure as for SUB42, but using an etchant solution with a $KI:I_2:H_2O$ molar ratio of 6:1:4. The profile face of the etched track was exposed by slicing the substrate with a sharp razor blade.

Figure B-3. Microscope photograph of Ag substrate SUB22 showing the profile view of a 1-mm wide etched track. The substrate thickness (measured vertically at the far left or right) is 127 μm.

Finally, note that the grain size of a polycrystalline Ag substrate before etching determines the roughness of the etched Ag surface. Silver that has been cold-worked (cold-rolled foil, for example) typically has a much smaller grain size than annealed silver and, therefore, a much smoother surface after etching. The samples of figures B-2 and B-3 are cold-rolled silver.

REFERENCES FOR APPENDIX B

Campbell, G. D., F. J. Lincoln, and I. M. Ritchie. 1986. "The Chemical Iodination of Silver," *Australian Journal of Chemistry*, vol. 39, p. 827.

Cotton, F. A. and G. Wilkinson. 1980. *Advanced Inorganic Chemistry*, 4th ed., ch. 22, p. 971, John Wiley and Sons, New York, NY.

Dahan, R., J. Dror, and N. Croitoru. 1992. "Characterization of Chemically Formed Silver Iodide Layers for Hollow Infrared Guides," *Materials Research Bulletin*, vol. 27, p. 761.

Peters, D. G., J. M. Hayes, and G. M. Hieftje. 1974. *Chemical Separations and Measurements*, ch. 10, p. 322, W. B. Saunders, Philadelphia, PA.

APPENDIX C: ARGON ANNEALING OF Bi2212

Any increase in the critical temperature of Bi2212 (or Bi2212+Ag) should produce a corresponding increase in the critical current density at a given temperature. A higher critical current in turn would lead to higher achievable magnetic fields for a magnet made from the superconductor. A Bi2212 sample made in air using the melt-processing techniques described in the EXPERIMENTAL RESULTS section typically has a T_c of around 80 K. As reported by various investigators, the Bi2212 T_c can be raised to about 92 K by optimizing the oxygen content of the compound (Peña *et al.*, 1989; Motoi *et al.*, 1989). For an air-processed sample, this requires that some oxygen be removed (Denia *et al.*, 1990; Triscone *et al.*, 1991). One way to do this is to anneal the sample in an inert gas at a temperature of a few hundred degrees centigrade (O'Bryan *et al.*, 1990).

A set of three anneals under flowing Ar were performed on a 1.7 mm × 2.1 mm × 2.0 cm bar sample (BCS663) of bulk Bi2212. The bar was cut from a pressed pellet prepared from the same Bi2212 powder batch as used for the melt-processed films, and sintered according to:

$$25 \xrightarrow{300\ ^\circ C/hr} \overset{15\ hr}{865} \xrightarrow{300\ ^\circ C/hr} 25\ ^\circ C \quad . \tag{C-1}$$

The four-probe resistivity of the sample was monitored *in situ* during the anneals (see MELT PROCESSING in the EXPERIMENTAL METHODS section), with the results shown in figures C-1 and 29. The time data for each anneal in figure C-2 have been shifted so that 0 hr corresponds to the beginning of the long, constant-temperature anneal. The first part of each anneal cycle was with the sample in air. For anneals 2 and 3, a flow of 99.998% argon gas through the furnace tube was started shortly after the anneal temperature was reached.

The low-temperature resistivity, measured after the above sintering cycle and after each subsequent anneal, is displayed in figures C-3 and C-4. Note that even though the post-anneal resistivity increased under conditions of both oxygen-loading (anneal 1, in air at 500°C) and oxygen-removal (anneal 2, in Ar after reaching 500°C), the sample showed a peak in T_c (presumably as a function of oxygen content). The peak in T_c (after anneal 2), therefore, does not correspond to the minimum resistivity (after sintering, but before any anneals). Note that the normal-state resistivity may be dominated by the intergranular, or weak-link, regions of these polycrystalline samples, while the main superconducting transition mainly reflects the character of the grains (Goldschmidt, 1989).

As mentioned in the subsection Bi2212 THICK FILMS ON MAGNESIUM OXIDE SUBSTRATES, thick-film sample FCS341 was annealed along with bulk Bi2212 sample BCS663 during anneal 3 (in Ar after reaching 600°C). As seen in the solid curve of figure C-5, the main resistive transition (corresponding to the T_c of the sample's grains) increased to about 91 K after this anneal. Application of this annealing technique to a Bi2212 thick-film magnet might, therefore, lead to improved performance. Note from the inset of the figure, however, that the zero resistance point (corresponding to the sample's intergranular T_c) is still about 83 K, the same as before the argon anneal. These data plots indicate that the T_c of the bulk material (within the grains) is improved by this 600°C anneal, but the T_c of the intergranular regions (between grains) is not. As seen in the bulk sample results of figure C-3, however, a 600°C anneal temperature may be too high. Note also that the bulk sample does not display the resistance transition "tail" that is seen in the thick-film sample. Optimization of the thick-film anneal temperature may eliminate this "tail" feature. Other methods of maximizing T_c in Bi2212, such as substitution of yttrium for calcium (see Narsaiah *et al.* and

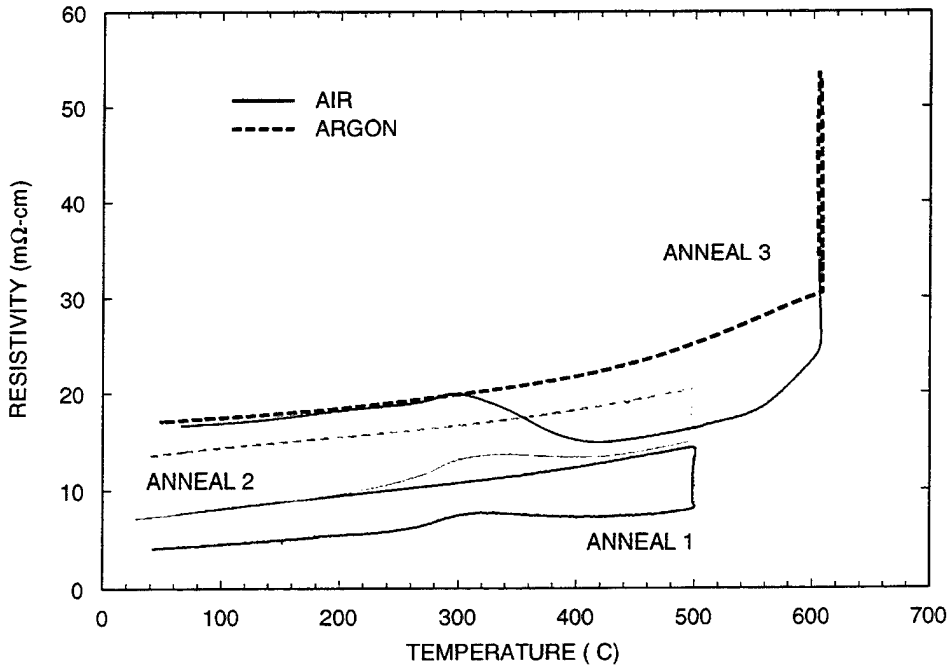

Figure C-1. Resistivity versus temperature for bulk Bi2212 sample BCS663 during three different anneal cycles. For anneals 2 and 3, the furnace atmosphere was switched from air to Ar after reaching the anneal temperature.

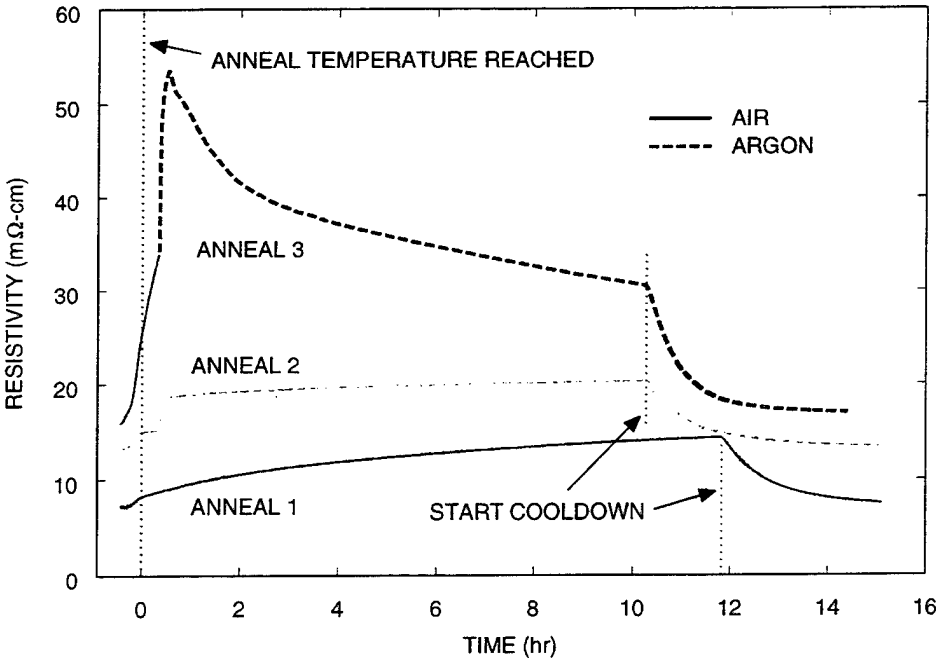

Figure C-2. Resistivity versus time for the three anneal cycles of bulk Bi2212 sample BCS663 shown in figure C-1.

references within; also Hu *et al.*, 1994), could also be used instead of inert gas anneals to improve spiral magnet performance.

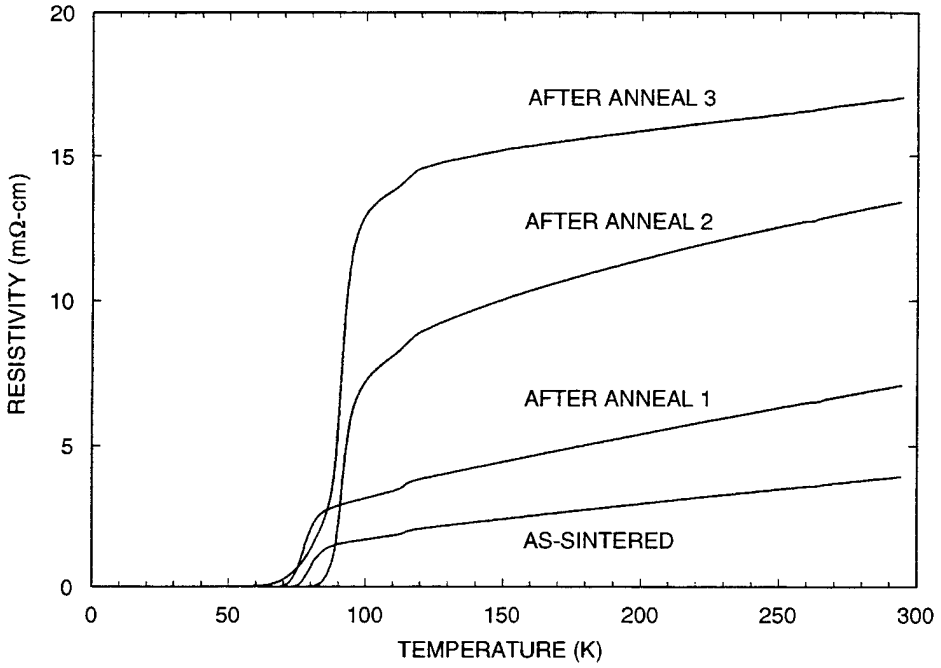

Figure C-3. Low temperature resistivity versus temperature for bulk Bi2212 sample BCS663 before (as-sintered) and after the three anneal cycles of figures C-1 and C-2.

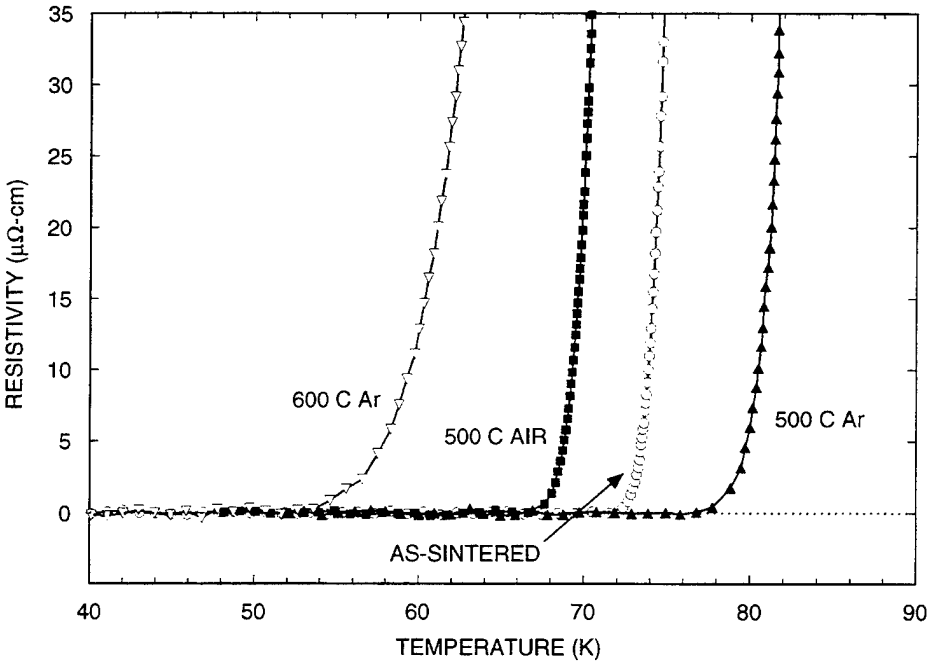

Figure C-4. Magnified view of the superconducting transitions shown in figure C-3 for bulk Bi2212 sample BCS663.

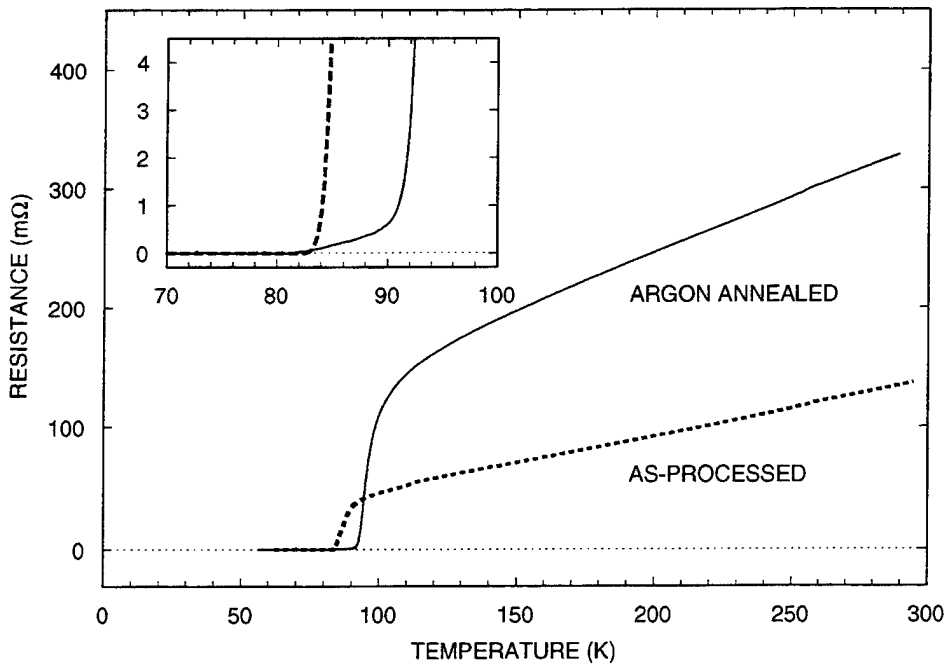

Figure C-5. As-processed (dashed) and post-Ar-anneal (solid) resistance versus temperature data for Bi2212 thick film FCS341 on an MgO substrate. The inset shows a magnified view of the superconducting transitions.

REFERENCES FOR APPENDIX C

Dinia, M. A., O. Peña, C. Perrin, and M. Sergent. 1990. "Enhancement of T_c and Reversible Effects by Annealing Undoped and Lead-Doped Bi-Sr-Ca-Cu Oxides," *Solid State Communications*, vol. 73, p. 715.

Goldschmidt, D. 1989. "Multiple Superconducting Transition in Ceramic $YBa_2Cu_3O_{7-\delta}$," *Physical Review B*, vol. 39, p. 2372.

Hu, D., V. Brabers, and W. J. M. de Jonge. 1994. "Effects of Partial Yttrium Substitution in $Bi_2Sr_2Ca_{1-x}Y_xCu_2O_{8+z}$ Single Crystals," *Physica C*, vol. 235-240, p. 951.

Motoi, Y., Y. Ikeda, H. Uwe, and T. Sakudo. 1989. "Enhancement of T_c by Annealing under Reducing Conditions on $Bi_2Sr_2CaCu_2O_x$," *Physica C*, vol. 162-164, p. 929.

Narsaiah, E. L., U. V. S. Rao, O. Peña, and M. Sergent. 1993. "Substitution Effects of Yttrium in the BISCCO (2212) System," *Materials Chemistry and Physics*, vol. 33, p. 58.

O'Bryan, H. M., W. W. Rhodes, and P. K. Gallagher. 1990. "Effect of Oxygen Stoichiometry on the Critical Temperature and Thermal Expansion of Two-Layer BiSrCaCu Oxide Superconductors," *Chemistry of Materials*, vol. 2, p. 421.

Peña, O., A. Dinia, C. Perrin, A. Perrin, and M. Sergent. 1989. "Reducing and Oxidizing Annealings of Bismuth High-T_c Superconductors," *Physica C*, vol. 162-164, p. 1215.

Triscone, G., J.-Y. Genoud, T. Graf, A. Junod, and J. Muller. 1991. "Variation of the Superconducting Properties of $Bi_2Sr_2CaCu_2O_{8+x}$ with Oxygen Content," *Physica C*, vol. 176, p. 247.

REPORT DOCUMENTATION PAGE

Form Approved
OMB No. 0704-0188

Public reporting burden for this collection of information is estimated to average 1 hour per response, including the time for reviewing instructions, searching existing data sources, gathering and maintaining the data needed, and completing and reviewing the collection of information. Send comments regarding this burden estimate or any other aspect of this collection of information, including suggestions for reducing this burden, to Washington Headquarters Services, Directorate for Information Operations and Reports, 1215 Jefferson Davis Highway, Suite 1204, Arlington, VA 22202-4302, and to the Office of Management and Budget, Paperwork Reduction Project (0704-0188), Washington, DC 20503.

1. AGENCY USE ONLY *(Leave blank)*	2. REPORT DATE	3. REPORT TYPE AND DATES COVERED
	April 1997	July 1995 to September 1996

4. TITLE AND SUBTITLE
High-T_c Superconducting Thick-Film Spiral Magnet:
Development and Characterization of a Single Spiral Module

5. FUNDING NUMBERS
PE: 0604561N
AN: DN302031
WU: D36–XB70

6. AUTHOR(S)
W. C. McGinnis, T. E. Jones

7. PERFORMING ORGANIZATION NAME(S) AND ADDRESS(ES)
Naval Command, Control and Ocean Surveillance Center (NCCOSC)
RDT&E Division
San Diego, California 92152–5001

8. PERFORMING ORGANIZATION REPORT NUMBER
TR 1741

9. SPONSORING/MONITORING AGENCY NAME(S) AND ADDRESS(ES)
Office of Naval Research
Code 01122
800 N. Quincy Street
Arlington, VA 22217

10. SPONSORING/MONITORING AGENCY REPORT NUMBER

11. SUPPLEMENTARY NOTES

12a. DISTRIBUTION/AVAILABILITY STATEMENT
Approved for public release; distribution is unlimited.

12b. DISTRIBUTION CODE

13. ABSTRACT *(Maximum 200 words)*

The objective of this project was to make characterized and numerically model prototype modules of a new type of superconducting electromagnet based on stacked spirals of superconducting thick films instead of solenoid-wound wires. Using the techniques reported in this document, a high-field magnet based on multiple stacked modules of interconnected high-T_c spiral thick films can be constructed and successfully operated. The magnetic fields produced by such an arrangement meet or exceed those predicted by a simple computer model of the magnet. Based on the measured field factor of a single 3.2-turn, 5-cm diameter module, a 2-cm long stack of 100 such modules, with a current-carrying capacity of 50 A, would produce maximum field of about 7.5 kOe. This, however, is not a limiting field for this magnet design, as much larger fields can be realized with higher current or by increasing the number of spiral turns.

14. SUBJECT TERMS
Mission area: Ocean Engineering
superconductivity
thick-film spiral magnets

15. NUMBER OF PAGES
58

16. PRICE CODE

17. SECURITY CLASSIFICATION OF REPORT	18. SECURITY CLASSIFICATION OF THIS PAGE	19. SECURITY CLASSIFICATION OF ABSTRACT	20. LIMITATION OF ABSTRACT
UNCLASSIFIED	UNCLASSIFIED	UNCLASSIFIED	SAME AS REPORT

21a. NAME OF RESPONSIBLE INDIVIDUAL	21b. TELEPHONE *(include Area Code)*	21c. OFFICE SYMBOL
W. C. McGinnis	(619) 553-5610	Code D364

INITIAL DISTRIBUTION

Code D0012	Patent Counsel	(1)
Code D0271	Archive/Stock	(6)
Code D0274	Library	(2)
Code D0271	D. Richter	(1)
Code D14	E. W. Hendricks	(1)
Code D30	F. E. Gordon	(1)
Code D364	W. C. McGinnis	(11)
Code D364	I. Stevens	(1)

Defense Technical Information Center
Fort Belvoir, VA 22060–6218 (4)

NCCOSC Washington Liaison Office
Washington, DC 20363–5100

Center for Naval Analyses
Alexandria, VA 22302–0268

Navy Acquisition, Research and Development
Information Center (NARDIC)
Arlington, VA 22244–5114

GIDEP Operations Center
Corona, CA 91718–8000

Naval Air Warfare Center Weapons Division
Mr. Donald R. Bowling, Code 4B1100D
China Lake, CA 93555–6001

Office of Naval Research
Mr. James E. Gagorik
Dr. Wallace A. Smith
Dr. Maribel Soto
Dr. Deborah Van Vechten
Arlington, VA 22217–5660 (4)

Naval Research Laboratory
Dr. Donald U. Gubser, Code 6300
Washington, DC 20375–5320

Naval Surface Warfare Center
Carderock Division
Mr. Owen Ritter, Code 2216
West Bethesda, MD 20817–5700 (5)